Biogeosciences

Spatial variability of organic matter molecular composition and elemental geochemistry in surface sediments of a small boreal Swedish lake

Julie Tolu[1], Johan Rydberg[1], Carsten Meyer-Jacob[1], Lorenz Gerber[2], and Richard Bindler[1]

[1]Department of Ecology and Environmental Science, Umeå University, 901 87 Umeå, Sweden
[2]Umeå Plant Science Center, Swedish University of Agricultural Sciences, Department of Forest Genetics and Plant Physiology, 901 83 Umeå, Sweden

Correspondence to: Julie Tolu (julietolu@hotmail.com)

Abstract. The composition of sediment organic matter (OM) exerts a strong control on biogeochemical processes in lakes, such as those involved in the fate of carbon, nutrients and trace metals. While between-lake spatial variability of OM quality is increasingly investigated, we explored in this study how the molecular composition of sediment OM varies spatially within a single lake and related this variability to physical parameters and elemental geochemistry. Surface sediment samples (0–10 cm) from 42 locations in Härsvatten – a small boreal forest lake with a complex basin morphometry – were analyzed for OM molecular composition using pyrolysis gas chromatography mass spectrometry for the contents of 23 major and trace elements and biogenic silica. We identified 162 organic compounds belonging to different biochemical classes of OM (e.g., carbohydrates, lignin and lipids). Close relationships were found between the spatial patterns of sediment OM molecular composition and elemental geochemistry. Differences in the source types of OM (i.e., terrestrial, aquatic plant and algal) were linked to the individual basin morphometries and chemical status of the lake. The variability in OM molecular composition was further driven by the degradation status of these different source pools, which appeared to be related to sedimentary physicochemical parameters (e.g., redox conditions) and to the molecular structure of the organic compounds. Given the high spatial variation in OM molecular composition within Härsvatten and its close relationship with elemental geochemistry, the potential for large spatial variability across lakes should be considered when studying biogeochemical processes in-volved in the cycling of carbon, nutrients and trace elements or when assessing lake budgets.

1 Introduction

In lake basins, a wide range of factors are known to influence the transport and fate of sedimentary material, such as the location of inlet streams, catchment topography, land-use patterns, fetch, basin morphometry and sediment focusing. Sediment focusing results from a combination of factors such as wind and wave action, basin slope and the settling velocity of different particle sizes, which all contribute to the redistribution of light, fine-grained material rich in clays, organic matter (OM) and associated trace elements from shallower to deeper waters (Blais and Kalff, 1995; Ostrovsky and Yacobi, 1999). While sediment focusing is important, catchment and lake characteristics can be complex and exert a primary influence on spatial patterns in sediment geochemistry, such as in relation to land use in near-shore areas (Dunn et al., 2008; Vogel et al., 2010; Sarkar et al., 2014), complex lake basin morphometries (Bindler et al., 2001; Rydberg et al., 2012) or river inflows (Kumke et al., 2005). The presence of macrophytes or wind-induced water currents have also been shown to affect the spatial distribution of lead (Pb), phosphorus (P) and OM (Benoy and Kalff, 1999; Bindler et al. 2001).

Because trace metals and nutrients are primarily associated with – or are part of – OM, studies focusing on the spatial patterns of metal or nutrient accumulation typically

include an analysis of the OM content. The two standard approaches to determine sediment OM content are the analysis of loss on ignition (LOI; Ball, 1964; Santisteban et al., 2004) or the analysis of elemental carbon (C). However, either approach inherently treats OM as a homogeneous sediment component. Recent studies interested in the role of lake sediments as a long-term C sink have likewise mainly treated OM and C as a homogeneous component (e.g., Sobek et al., 2003; Tranvik et al., 2009; Heathcote et al., 2015). Even if this approach is rational from a global perspective of calculating C budgets, treating OM as a homogeneous component is overly simplistic from the perspective of developing insights into the biogeochemical behavior of OM and its influence on C, nutrient, and trace metal cycling and does not take full advantage of the information provided by differences in the OM quality.

In boreal lakes the sediment composition is often dominated by OM, typically ranging from 20 to 60 % on a dry weight basis. Biogenic silica (bSi) may account for as much as 45 % of the sediment dry weight (Meyer-Jacob et al., 2014), and the remaining sediment mainly consists of detrital mineral matter and possibly authigenic minerals. Lake OM is an extremely heterogeneous and complex mixture of molecules that are derived from residues of plants, animals, fungi, algae and microorganisms, which are either transported into the lake from the surrounding catchment (allochthonous) or produced within the lake (autochthonous). Furthermore, these organic compounds may undergo transformations within the water column and the sediment through both biotic and abiotic processes. There have been a few studies where the spatial complexity in OM quality within a lake basin has been assessed using infrared spectroscopy, which yields qualitative information on variations in OM quality (Korsman et al., 1999; Rydberg et al., 2012), or quantitative analyses of photopigments and lipids (Ostrovsky and Yacobi, 1999; Trolle et al., 2009; Vogel et al., 2010; Sarkar et al., 2014). However, little work has been done to detail how the molecular composition of the sediment OM matrix varies spatially within a lake, considering a large number of organic biochemical classes and compounds.

To characterize OM composition at the molecular level, the most commonly used methods are based on liquid or gas chromatography (LC or GC) coupled to fluorescence or mass spectrometry (MS) detection. These methods provide quantitative data on original organic compounds found in the analyzed samples, including highly specific biomarkers of OM sources, for example, and have been successfully employed to study OM composition and reactivity in environmental matrices as well as to reconstruct environmental changes (e.g., changes in vegetation, algal productivity) from peat or sediment cores. However, the associated sample preparation procedures, i.e., extraction–hydrolysis and derivatization, are fastidious and specific to the different biochemical classes of organic compounds such as carbohydrates, proteins or amino acids, lipids, chlorophylls and lignin (e.g.,

Wakeham et al., 1997; Dauwe and Middelburg, 1998; Tesi et al., 2012). Moreover, sample masses > 10 mg are required. Hence, studies where different OM biochemical classes are targeted using these wet chemical extraction and GC/LC–MS methods are very scarce. However, efforts in characterizing the whole OM composition at the molecular level can bring important insights because the different biochemical classes of OM do not always include specific biomarkers for the different existing sources of OM (e.g., terrestrial plants, macrophytes, higher plants, mosses, algae, bacteria). For example, lignin oligomers are only specific of higher plants (Meyer and Ishiwatari, 1997) and proteins and amino acids mainly provide biomarkers for bacteria and planktonic production (Bianchi and Canuel, 2011). Moreover, the different biochemical classes of OM do not present the same reactivity; for example, proteins, amino acids and neutral carbohydrates have been shown to be among the most reactive organic molecules (e.g., Fichez, 1991; Dauwe and Middelburg, 1998; Amon and Fitznar, 2001; Tesi et al., 2012). Advanced ultra-high-resolution MS techniques, i.e., Fourier transform ion cyclotron resonance mass spectrometry (FT-ICR-MS) or linear trap quadruple Orbitrap MS, enable the determination of a large number of organic molecular formulas in liquid samples (> 1000; e.g., Hawkes et al., 2016). These methods have been successfully used to link variability in the molecular composition of dissolved OM (DOM) with different factors and/or processes of environmental ecosystems, such as climate, hydrology and OM degradation in boreal lakes (Kellerman et al., 2014, 2015) or optical properties and DOM photochemical alterations in wetland and seawater (Stubbins and Dittmar, 2015; Wagner et al., 2015). However, in addition to the limited access to these advanced MS techniques due to instrumental costs, extraction–hydrolysis steps are required when studying solid samples, which also make these methods specific to the different biochemical classes of organic compounds.

To study the variability of OM composition in sediments, pyrolysis gas chromatography mass spectrometry (Py–GC–MS) is a good compromise between (i) the quantitative LC/GC–MS or the high-resolution MS methods that target specific compounds and (ii) the qualitative, nonmolecular information provided by high-throughput techniques such as infrared spectroscopy or "Rock-Eval" pyrolysis. Py–GC–MS analysis requires no complex sample preparation but yields semiquantitative data on > 100 organic compounds that are chemical fingerprints of the different OM biochemical classes, which include specific biomarkers for OM sources and degradation status (Faix et al., 1990, 1991; Peulvé et al., 1996; Nierop and Buurman, 1998; Schulten and Gleixner, 1999; Lehtonen et al., 2000; Nguyen et al., 2003; Page, 2003; Buurman et al., 2005; Fabbri et al., 2005; Kaal et al., 2007; Vancampenhout et al., 2008; Schellekens et al., 2009; Carr et al., 2010; Buurman and Roscoe, 2011; De La Rosa et al., 2011; McClymont et al., 2011; Micić et al., 2011; Stewart, 2012).

In the present study, we apply our newly optimized Py–GC–MS method to characterize the molecular composition of natural OM in surface sediments (0–10 cm) from 42 locations within the lake basin of Härsvatten. Härsvatten is a small boreal forest lake in southwestern Sweden that was previously studied for the spatial distribution of Pb and OM contents (Bindler et al., 2001). Our objective here was to comprehensively investigate how the molecular composition of sediment OM varies spatially across a lake with several basins. Our specific research questions were (i) what are the spatial patterns within a single lake for various organic biochemical classes and compounds? (ii) How does the spatial pattern of the OM molecular composition relate to physical parameters (i.e., bulk density and water depth) and elemental, inorganic geochemistry of the sediment material? (iii) Which factors or processes (e.g., provenance, transport pathway and mineralization) appear to explain the in-lake spatial variability of the OM molecular composition?

2 Materials and methods

2.1 Study site and samples

Härsvatten is a boreal forest lake located in southwestern Sweden (58°02′ N, 12°03′ E) in the Svartedalen nature reserve. This culturally acidified, clear-water, oligotrophic and fishless lake has been intensively monitored since the 1980s (national database, Department of Aquatic Sciences and Assessment, Swedish University of Agricultural Sciences, Uppsala, Sweden; www.slu.se), during which time the pH has ranged from 4.2–4.5 in 1983–1987 to 4.7–5.6 in 2010–2014. The lake is dimictic with a thermal stratification between 10 and 15 m depth in the summer. Approximately 80 % of the lake bottom is within the epilimnion. The surface areas of the lake and its catchment are 0.186 and 2.03 km^2, respectively. The catchment is characterized by an uninhabited, coniferous-dominated forest (*Picea abies* Karst. and *Pinus sylvestris* L.), which extends to the rocky shoreline. The bedrock consists of slow-weathering granites and gneisses that are covered by thin and poorly developed podsolic soils.

The basin of Härsvatten can be divided into four general areas (Bindler et al., 2001): (1) the main south basin, which represents about half of the lake area (sample sites S1–S24; maximum depth, 24.3 m) and includes the lake's small outlet stream; (2) a north basin (sample sites N1–11; maximum depth, 12 m), which includes a small inlet stream draining from the headwater lake Måkevatten that enters Härsvatten through a small wetland; (3) an east basin, which has a maximum depth of nearly 10 m (sample sites E1–E6) and is separated from the main north–south axis of the lake by a series of islands and shallow sills (< 3 m water depth); and (4) a generally shallow (< 3 m water depth) central area separating the north, east and south basins (sample sites M1–M6).

In total, we analyzed 44 surface sediment (0–10 cm) samples that were collected in winter 1997–1998 (Fig. 1) for a study of Pb and spheroidal carbonaceous particles (Bindler et al., 2001). These samples were collected as follows: short sediment cores (0–25 cm) were taken with a gravity corer from the ice-covered lake in winter 1997 and 1998 and were sectioned on-site into an upper sample (0–10 cm) and a lower sample (10–25 cm; not studied here). In the laboratory, the samples were weighed, freeze-dried, and reweighed to determine the water content and dry mass of the sediment. The freeze-dried samples have been stored in plastic containers within closed boxes shielded from light and at room temperature since winter 1997–1998. Before further analysis in this study, the samples were finely ground at 30 Hz for 3 min using a stainless steel Retsch swing mill.

2.2 Major and trace element concentrations

The concentrations of major (Na, Mg, Al, Si, K, Ca, P, S, Mn, Fe) and trace elements (Sc, Ti, V, As, Br, Y, Zr, Ni, Cu, Zn, Sr, Pb) were determined using a wavelength-dispersive X-ray fluorescence spectrometer (WD-XRF; Bruker S8 TIGER) and a measurement method developed for powdered sediment samples (Rydberg, 2014). Accuracy was assessed using sample replicates, which were within ±10 % for all elements.

Total mercury (Hg) concentrations were determined using thermal desorption atomic absorption spectrometry (Milestone DMA-80) with the calibration curves based on analyses of different masses of four certified reference materials (CRMs). Analytical quality was controlled using an additional CRM and replicate samples included with about every 10 samples. The CRM was within the certified range, and replicate samples were within ±10 % for Hg concentrations < 30 µg kg^{-1} and within ±5 % for concentrations ≥ 30 µg kg^{-1}.

We also included the OM content (in % dry mass), determined as LOI after heating dried samples at 550 °C for 4 h in the earlier study of Bindler et al. (2001).

2.3 Biogenic silica concentrations

Biogenic silica (bSi) was determined by Fourier transform infrared (FTIR) spectroscopy following the approach described in Meyer-Jacob et al. (2014). In brief, sediment samples were mixed with potassium bromide (0.011 g sample and 0.5 g KBr) prior to analysis with a Bruker VERTEX 70 equipped with a HTS-XT accessory unit (multi-sampler). The recorded FTIR spectral information was used to determine the bSi concentrations employing a partial least squares regression (PLSR) calibration based on analyses of synthetic sediment mixtures with defined bSi content ranging from 0 to 100 %.
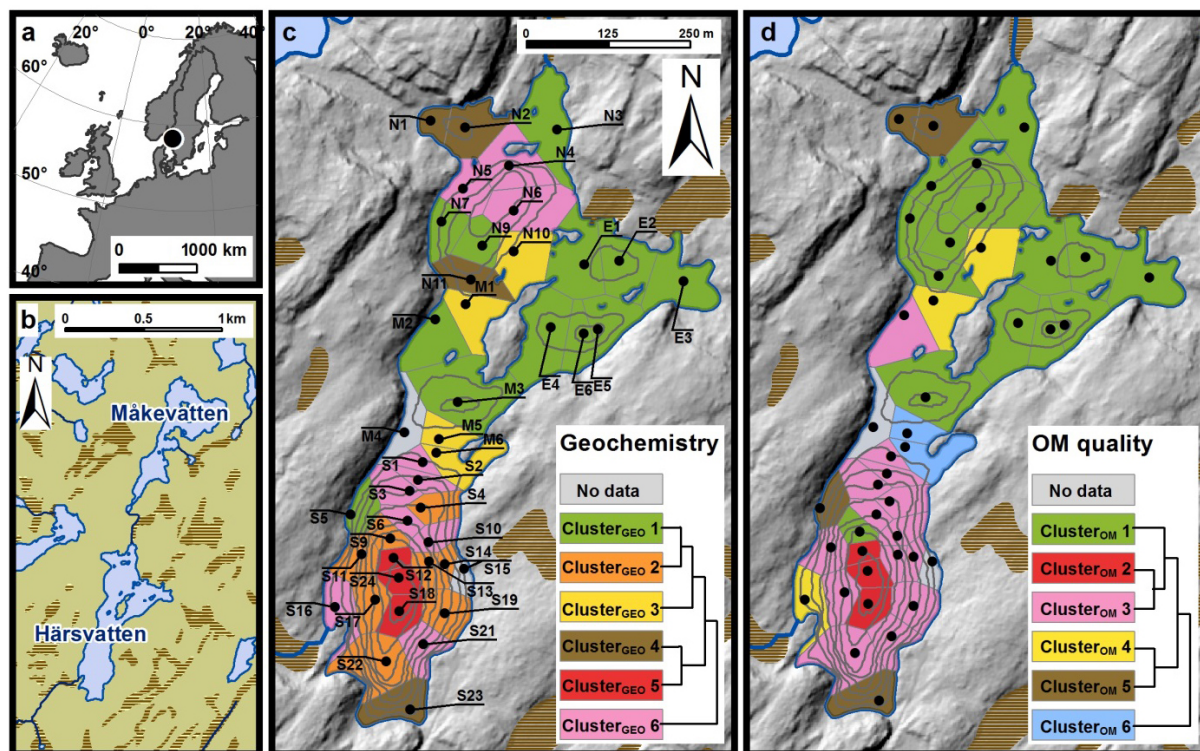
Figure 1. Maps of Härsvatten showing **(a)** its location in Europe; **(b)** its catchment with lakes, mires and larger streams; and **(c, d)** its bathymetry along with the spatial distribution of the 44 sampling sites and the six selected clusters based on sediment elemental geochemistry **(c)** and sediment OM molecular composition **(d)**. In **(c)** and **(d)**, the dendrogram shows the relationship between the six identified clusters.

We calculated the mineral Si fraction ($Si_{mineral}$) from the difference between the total Si concentration determined by WD-XRF (Sect. 2.2) and the bSi concentration.

2.4 Organic matter molecular composition

The molecular composition of OM was determined by Py–GC–MS following the method developed by Tolu et al. (2015). In brief, $200 \pm 10 \mu g$ sediment was pyrolyzed in a Frontier Labs PY-2020iD oven ($450 °C$) connected to an Agilent 7890A-5975C GC–MS system. Peak integration was done using a data processing pipeline under the "R" computational environment. Peak identification was made using the software "NIST MS Search 2" containing the library "NIST/EPA/NIH 2011" and additional spectra from published studies.

In the sediments of Härsvatten, 162 pyrolytic organic compounds were identified, and peak areas were normalized by setting the total identified peak area for each sample to 100 %. A detailed list of the 162 identified organic compounds is provided in the supplementary information along with information on their molecular mass and structure, references for the theoretical mass spectra and calculated or reference retention index values (Table S1 in the Supplement). Although the pyrolysis temperature we employed, i.e.,

$450 °C$ as used in plant science (e.g., Faix et al., 1990; Faix et al., 1991), is different from the pyrolysis temperature that was most commonly used for analyzing soils, sediments, peat records and algae (i.e., $> 600 °C$), our list is highly similar to published lists of identified pyrolytic organic compounds both in terms of the organic compounds and of their classification into 13 OM classes (Faix et al., 1990, 1991; Peulvé et al., 1996; Nierop and Buurman, 1998; Schulten and Gleixner, 1999; Lehtonen et al., 2000; Nguyen et al., 2003; Page, 2003; Buurman et al., 2005; Fabbri et al., 2005; Kaal et al., 2007; Vancampenhout et al., 2008; Schellekens et al., 2009; Carr et al., 2010; Buurman and Roscoe, 2011; De La Rosa et al., 2011; McClymont et al., 2011; Micić et al., 2011; Stewart, 2012). Pyrolysis at $450 °C$ is preferred to pyrolysis at $650 °C$ when using very small sample mass (few hundred micrograms) because it avoids complete degradation of some specific biomarkers of OM sources and enables determination of OM degradation status by identification of levosugars (pyrolytic products of polysaccharides and/or cellulose) or syringol lignin oligomers, for instance (Tolu et al., 2015).

2.5 Statistical analysis

We performed all statistical analyses using SPSS software package PASW, version 22.0. Two separate principal compo-

nent analyses (PCA) were performed, one for the elemental geochemistry (i.e., dry bulk density (B.D.) and contents of OM (LOI), major and trace elements, and bSi) and the other for the OM molecular composition. Prior to the PCA, all data were converted to Z-scores (average = 0, variance = 1). Principal components (PCs) with eigenvalues > 1 were retained and extracted using a Varimax rotated solution. Factor loadings were calculated as regression coefficients, which is analogous to r in Pearson correlations. For convenience the loadings are reported as percentage of variance explained, i.e., as squared loadings. For all PCs, variables with squared loadings < 0.15 are not discussed with respect to that PC. Other variables, e.g., water depth (W.D.) or ratios between elements, were included passively in the PC-loading plots by using bivariate correlation coefficients between these variables and the PC scores of each PC. Hierarchical agglomerative cluster analysis (CA) was performed for the elemental geochemistry and the OM molecular composition datasets using Ward's linkages (Ward, 1963) based on squared Euclidean distances. The PC scores from the PCAs were used instead of the original data in order to eliminate the effects of autocorrelation in the dataset.

3 Results and discussion

3.1 Sediment elemental geochemistry

3.1.1 General description and trends

Summary statistics of the elemental geochemical properties of the surface sediments from Härsvatten are presented in Table 1 and the detailed data are given in Table S2. The sediments from sites M4 and S15 are two outliers because they have B.D., bSi, OM and elemental contents (e.g., Na, Mg, Al, K) that deviated by more than 4 standard deviations from the average values of all analyzed sediment samples (Table 1). Moreover, these sediment samples are too coarse (predominantly sand) for Py–GC–MS analysis according to our method based on $200 \pm 10\,\mu g$ analyzed sample mass. Hence, they are excluded from the statistical analyses and discussion. Even when excluding these two sites, the elemental geochemical parameters vary considerably across the lake basin, with Hg, Fe, Co and Mn contents illustrating the greatest variabilities (i.e., coefficients of variation, CVs > 60 %) and Al, Br, K, Ti, V, Ni, Mg and Ca contents showing the lowest variabilities (CVs: 17–25 %; Table 1). For most geochemical properties, the average to median ratios are approximatively 1.0, indicating no extreme values. Slightly higher values were, however, observed for P, Fe, As and Co contents (1.2–1.3), and Mn content is associated with extremely large values outside the population distribution (average : median = 4.1).

The lowest B.D. is observed among the three deepest sampling locations (23.5–24.5 m) in the main south basin, where

we also find the lowest bSi content and the highest contents in organically bound elements, including S, Br, P and certain trace metals, i.e., Cu, Ni, Hg and Zn. These sediments have high OM content (> 50 %), but the highest [OM] (57–58 %) are observed among isolated sites that are located close to the shoreline (N1–N2, E3, S5, S23; 3.1–7.4) and that also include the lowest [Al], [P], [K], [Si$_{inorganic}$], [V] and [Zr]. The highest B.D. and the lowest [OM], [S], [Br], [Cu], [Ni], [Hg] and [Zn] are observed among the shallow sites (1.8–2.5 m) located between the north and east basins and between the larger north and south basins (i.e., sites N10, M1, M5–M6), which also contain the highest [bSi], [Sr], [Al], [Y], [Mn] and [Co]. The sediments located at intermediate water depth (9–20 m) in the main south basin (S4, S9, S11, S13–14, S17, S19, S22) are associated with the highest [Fe], [As], [K], [Mg], [Na], [Ti] and [Zr], while among the shallower sites of the south basin we find the highest [Si$_{inorganic}$]. The lowest [Fe], [As], [Co] and [Y] are observed among the sediments of the east basin, and the sediments of the north basin include the lowest [Mn], [Ca], [K], [Mg], [Na], [Sr] and [Zr]. To identify the most significant relationships between the different elemental geochemical properties and to more precisely explore their spatial distribution, the results of PCA and cluster analyses are further presented and discussed.

3.1.2 Principal components of the elemental geochemistry

For the elemental geochemistry dataset, five principal components were retained. We present only the first four PCs, which together explain 74 % of the total variance (PC1–4$_{geo}$; Fig. 2), because no reasonable interpretation could be made for PC5$_{geo}$ (10 % of the total variance; Fig. S1). PC1$_{geo}$ captures 25 % of the total variance and separates bSi and B.D. (negative loadings) from OM, S, Cu, Hg, Ni, Zn and, to a lesser extent, As and Pb (positive loadings, Fig. 2a). This means that bSi and B.D. are significantly positively correlated, and both are significantly negatively correlated to OM, S, Cu, Hg, Ni, Zn and, to a lesser extent, As and Pb. If those parameters do not have significant loadings on PC2–5, it means that they are not significantly correlated with the parameters found on PC2–5, the PCs being orthogonal to each other. The negative loadings on PC1 are interpreted as reflecting a bSi-rich fraction, while positive loadings indicate an organic-rich fraction that is enriched in organophilic trace metals (Lidman et al., 2014). For PC2$_{geo}$, which captures 21 % of the total variance, Si$_{inorganic}$, K, Na, Mg, Zr and Ti have positive loadings, while no element is significantly negatively correlated to PC2$_{geo}$ (Fig. 2a). High PC2$_{geo}$ scores likely represent samples that are richer in silicate minerals such as quartz and clays (Koinig et al., 2003; Taboada et al., 2006).

Positive loadings on PC3$_{geo}$, which explains 16 % of the total variance, are found for Al and Fe along with As, P and Y (Fig. 2b). Compared to elements such as Mg, Na

Table 1. Summary statistics for sediment elemental geochemistry.

	Unit	Whole sample collection except for the two outliers					Outliers (M4, S15)			
		Av.[a] ± SD[b]	CV[c]	Median	A : M[d]	Min[e]–max[f]	Av.[a] ± SD[b]	CV[c]	Median	Min[e]–max[f]
W.D.	m	9 ± 7	74	7	1.23	2–25	3.4 ± 0.6	19	3	2.9–3.8
B.D.	$g\,cm^{-3}$	0.06 ± 0.02	38	0.06	1.05	0.02–0.13	0.67 ± 0.09	14	0.06	0.61–0.74
bSi	%	13 ± 6	48	12	1.05	4–25	1.9 ± 0.2	0	12	1.7–2.0
LOI	%	38 ± 10	26	37	1.01	10–58	3.6 ± 0.8	20	37	3.0–4.1
[S]	$mg\,kg^{-1}$	11876 ± 5920	50	11 305	1.05	4685–29 190	2570 ± 552	21	10 610	2180–2960
[Br]	$mg\,kg^{-1}$	149 ± 35	23	152	0.99	71–225	16 ± 7	44	148	11–21
[Cu]	$mg\,kg^{-1}$	34 ± 13	37	32	1.07	12–75	9 ± 3	31	31	7–11
[Ni]	$mg\,kg^{-1}$	19 ± 4	24	19	0.99	10–27	12 ± 4	35	19	9–15
[Hg]	$\mu g\,kg^{-1}$	337 ± 202	60	286	1.18	117–1152	28 ± 9	33	274	21–34
[Pb]	$mg\,kg^{-1}$	192 ± 74	39	184	1.05	58–422	22 ± 16	76	178	10–33
[Zn]	$mg\,kg^{-1}$	219 ± 108	49	207	1.06	43–445	50 ± 16	31	200	39–61
[Al]	%	3 ± 1	17	3	1.06	2–4	5.67 ± 0.01	0.1	3	5.66–5.67
[Y]	$mg\,kg^{-1}$	25 ± 8	32	25	1.01	7–43	20 ± 4	18	25	17–22
[Fe]	%	5 ± 3	65	4	1.26	1–12	3.4 ± 0.1	4	4	3.3–3.5
[As]	$mg\,kg^{-1}$	35 ± 20	56	28	1.26	5–73	< DL		27	0–0
[P]	$mg\,kg^{-1}$	1624 ± 741	46	1401	1.16	655–3769	949 ± 57	6	1389	908–989
[Mn]	$mg\,kg^{-1}$	729 ± 1690	232	180	4.06	94–7981	1060 ± 845	80	184	462–1657
[Co]	$mg\,kg^{-1}$	19 ± 15	77	14	1.39	5–76	17 ± 9	56	14	10–23
[Ca]	$mg\,kg^{-1}$	5261 ± 1306	25	5213	1.01	2860–9300	$26\,540 \pm 7566$	29	5283	21 190–31 890
[K]	$mg\,kg^{-1}$	4426 ± 1020	23	4485	0.99	2420–6140	$10\,510 \pm 2616$	25	4580	8660–12 360
[Mg]	$mg\,kg^{-1}$	1488 ± 354	24	1500	0.99	870–2130	7495 ± 3599	48	1515	4950–10 040
[Na]	$mg\,kg^{-1}$	1795 ± 659	37	1743	1.03	440–3380	$10\,695 \pm 587$	5	1783	10 280–11 110
[Si$_{inorganic}$]	%	11 ± 4	33	11	1.06	4–21	23 ± 1	3	11	22–23
[Sr]	$mg\,kg^{-1}$	55 ± 16	29	55	1.01	27–116	235 ± 24	10	55	218–252
[Ti]	$mg\,kg^{-1}$	2115 ± 495	23	2200	0.96	997–2870	4357 ± 2348	54	2215	2697–6017
[V]	$mg\,kg^{-1}$	63 ± 15	23	60	1.05	36–101	75 ± 23	31	60	58–91
[Zr]	$mg\,kg^{-1}$	101 ± 31	31	100	1.01	39–160	158 ± 6	4	103	153–162

[a] Av.: average. [b] SD: standard deviation. [c] CV: coefficient of variation calculated as relative standard deviation in %. [d] A : M: ratio between average and median. [e] Min.: minimal value. [f] Max.: maximal value.

and K that are mostly confined to the silicate fraction of sediments, Fe and Al may reflect both detrital material and dissolved or amorphous phases. However, the fact that As and P contents as well as the Fe : Al ratio plot together with Fe and Al contents on the positive side of PC3$_{geo}$ and not with the S content strongly suggests that sediments with high PC3$_{geo}$ scores are associated with higher contents of Fe and Al (oxy)hydroxides, which are known to strongly bind both As and P (Mucci et al., 2000; Plant et al., 2005; Zhu et al., 2013). PC4$_{geo}$ captures 12 % of the total variance and separates Mn, Co, Pb and to a lesser extent Fe (positive loadings) from OM and Br (negative loadings; Fig. 2b). Although Mn, like Fe and Al, is not confined to a specific mineral phase and can reflect both detrital or dissolved and amorphous phases, the positive loadings are interpreted as reflecting Mn (oxy)hydroxides, which bind Pb, especially when they contain cobalt (Co) (Yin et al., 2011). This interpretation is supported by the positive loadings on PC4$_{geo}$ of the ratio Mn : Fe, often used as a paleolimnological proxy for bottom-water oxygenation (Naeher et al., 2013). The negative loadings could indicate a terrestrial OM fraction that is rich in Br (Leri and Myneni, 2012).

3.1.3 Cluster analysis of the elemental geochemistry

For the cluster analysis of the elemental geochemistry dataset, we selected a solution of six clusters (cluster$_{geo}$ 1–6, Fig. 1c). The cluster averages and standard deviations of each physical and geochemical variable are given in Table S3 where they are compared to the average values of all analyzed sediment samples, hereafter referred as the "whole-lake average". Table 3 provides the cluster averages for a selection of geochemical parameters.

In the south basin, the sediments found at shallower water depth (cluster$_{geo}$ 6, $n = 10$) have a higher B.D., are richer in bSi (negative scores on PC1$_{geo}$, Fig. 2a) and have lower than whole-lake average trace metal concentrations (Table 1). In contrast, the sediments from the deeper sites (cluster$_{geo}$ 5, $n = 3$) have the lowest B.D. and lowest bSi content (Table 1) and are enriched in OM and trace metals (positive scores on PC1$_{geo}$, Fig. 2a). The sediments found at intermediate water depths (cluster$_{geo}$ 2, $n = 8$) have positive scores on PC2$_{geo}$ (Fig. 2a), and they have an OM content within 10 % of the whole-lake average, while trace metal concentrations are above 10 % of the whole-lake averages (Table 1). The south basin as a whole has higher P concentrations than
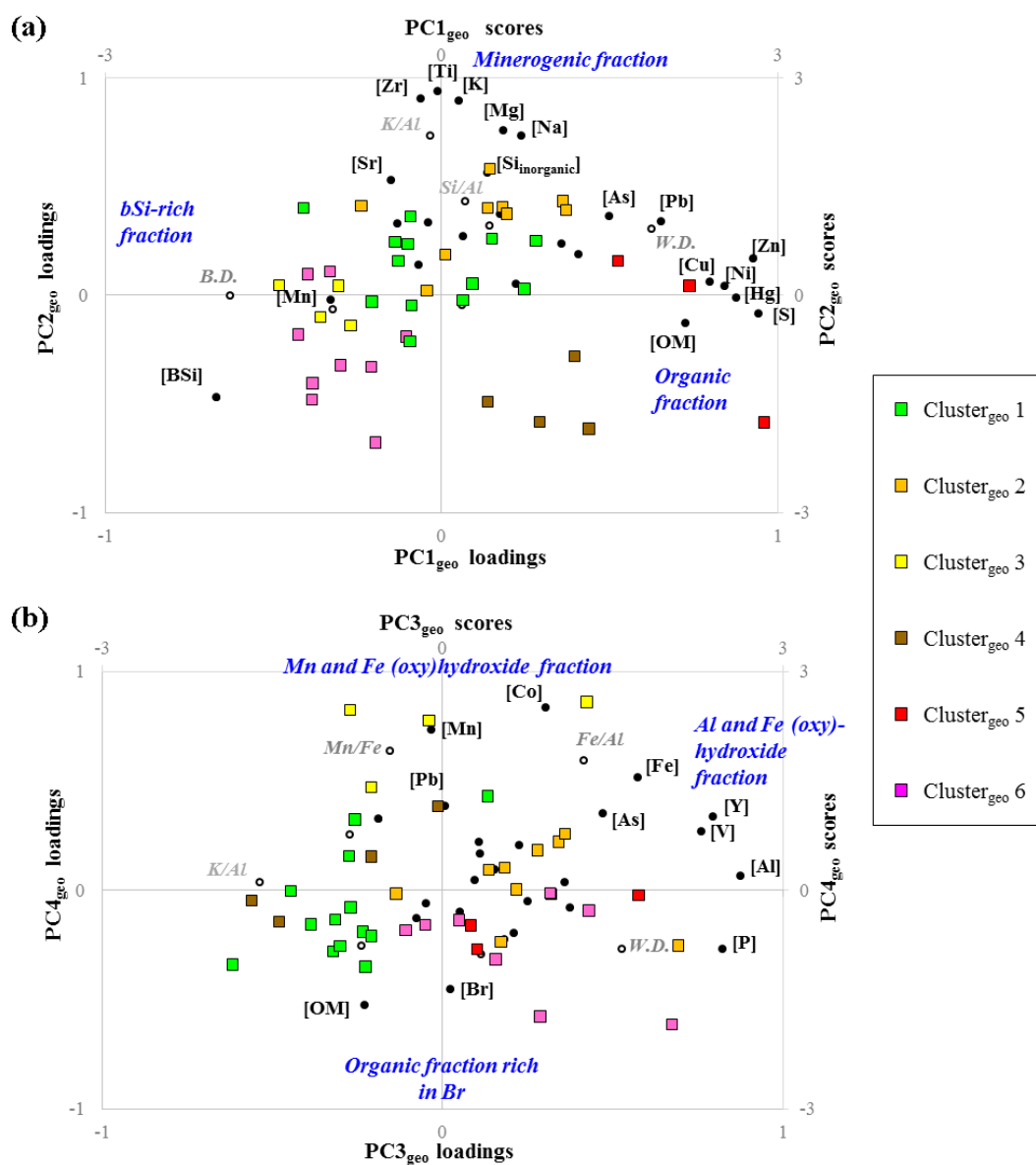
Figure 2. Combined loading and score plots for PCs 1–4 of the elemental geochemistry dataset. For the PC loadings, filled circles correspond to active variables. Other variables (empty circle and italics) were added passively. Sediment samples are colored according to the results of the cluster analysis.

the north, east and central areas, and in both intermediate and deeper sites the sediments are rich in Fe and As (positive scores on $PC3_{geo}$, Fig. 2b and Table 1).

The sediments found at shallow water depth between the north and east basins and in the central area (cluster$_{geo}$ 3, $n = 4$) have the highest B.D. and are the most enriched in both bSi (negative score on $PC1_{geo}$, Fig. 2a) and Mn and Fe (oxy)hydroxides (positive score on $PC4_{geo}$, Fig. 2b). A small number of shallow near-shore sampling locations (cluster$_{geo}$ 4, $n = 4$) have higher OM concentrations than the whole-lake average and are enriched in sulfur and trace metals (positive scores on $PC1_{geo}$, Fig. 2a and Table 1).

3.2 Sediment organic matter molecular composition

3.2.1 General description and trends

The pyrolytic products identified in the surface sediments of Härsvatten were classified into 13 OM classes, i.e., carbohydrates, N compounds, chitin-derived pyrolytic products, phenols, lignin, chlorophylls, *n*-alkenes, *n*-alkanes, alkan-2-ones, steroids, tocopherols, hopanoids and (poly)aromatics, in agreement with previous studies using Py–GC–MS for different environmental matrices (Faix et al., 1990, 1991; Peulvé et al., 1996; Nierop and Buurman, 1998; Schulten

and Gleixner, 1999; Lehtonen et al., 2000; Nguyen et al., 2003; Page, 2003; Buurman et al., 2005; Fabbri et al., 2005; Kaal et al., 2007; Vancampenhout et al., 2008; Schellekens et al., 2009 ;Carr et al., 2010; Buurman and Roscoe, 2011; De La Rosa et al., 2011; McClymont et al., 2011; Mićić et al., 2011; Stewart, 2012). For the sake of making the presentation of the data and the associated discussion more constrained and avoiding overinterpretation of individual compounds, the 162 identified organic compounds were reduced to 41 groups of compounds as described in Table 2. This grouping is based on similarities in the molecular structure within the OM classes (see Table S1), and preliminary principal component analyses have shown that the compounds within each of our 41 groups are highly positively correlated and thus present the same trends in our study (data not shown). As an example, the 20 identified carbohydrate compounds, previously demonstrated to derive from pyrolysis of polysaccharides and carbohydrates (Faix et al., 1991), have been separated into six groups based on the number of C in the heterocycles of these compounds and on their side-chain functional groups. The heterocycle of "furan" and "furanone" compounds contains four C atoms and one oxygen (O) atom, and the side-chain is either aliphatic ((alkyl)furans and (alkyl)furanones) or contains an oxygenated functional group (hydroxy- or carboxy-furans and furanones). While the heterocycle of "pyran" compounds has five C atoms and one O atom, the heterocycle of dianhydrorhamnose, levoglucosenone and levosugars consists of six C and one O. However, the levosugars contain three hydroxyl functional groups whereas dianhydrorhamnose contains two hydroxyl groups and levoglucosenone has a carbonyl group instead.

Summary statistics of these 41 groups of organic compounds are presented in Table 2 and the detailed data are given in Table S4. The coefficients of variation for the abundances of the different organic compound groups range from 15 to 106 % with an average of 38 ± 20 %, showing a remarkable in-lake variability of OM molecular composition. For most of the organic compound groups, the average to median ratios are approximatively 1.0, indicating no extreme values. However, slightly higher values (1.2–1.8) are observed for organic compounds derived from higher plants and mosses, i.e., levosugars, lignin oligomers (syringols and guaiacols), n-alkanes C25–C35, alkan-2-ones C23–C31 and tocopherols.

Most of the N compounds, which usually derive more from algae than from higher plants and mosses (Bianchi and Canuel, 2011), have the highest abundances among the three deepest sampling locations (23.5–24.5 m) in the main south basin (S12, S18 and S24). These three deepest sampling locations also present the highest abundances of (i) pyrolytic compounds containing an acetamide functional group previously shown to be a good indicator of the presence of chitin, a component of fundi cell walls and arthropod exoskeletons, in biological and geological samples (Gupta et al., 2007); (ii) phytadienes, i.e., pyrolytic products of chloro-

phylls (Nguyen et al., 2003); (iii) short-chain alkan-2-ones (2K C13–C17); and (iv) steroids. In contrast, most of the carbohydrates, which usually derive mostly from higher plants and mosses (Bianchi and Canuel, 2011), have the highest abundances among the sediments situated close to the shoreline (N1–N2, E3, S5, S23) such as for the abundances of phenols, guaiacyl- and syringyl-lignin oligomers, long-chain n-alkenes (C27–C28 : 1) and diketodipyrrole (N compounds), all specific of higher plant and/or moss OM (Meyers and Ishiwatari, 1993; Schellekens et al., 2009). The highest abundances of long-chain n-alkanes (C23–C26 : 0 and C27–C35 : 0) and mid-chain n-alkanes (C17–C22 : 0) are, however, observed for the shallower sites (< 2 m) situated between the larger north and south basins (sites M5–M6).

Among the shallow sites (2.5–3.0 m) located between the north and east basins (N10, M1) and the shallow and intermediate water depth (4–20 m) sites of the south basin (S1–S4, S6–S11, S13–S17, S19–S22), we find the highest abundances of degradation products of carbohydrates (i.e., (alkyl)furans and furanones and hydroxyl- or carboxy-furans and furanones); of proteins, amino-acids and/or chlorophylls (i.e., pyridines_O, (alkyl)pyrroles, pyrroles_O, pyrroledione and pyrrolidinedione, pristenes); and of lipids (i.e., short-chain n-alkenes and n-alkanes; C9–C16 : 1 and C13–C16 : 0) as well as the highest abundances of (poly)aromatic compounds indicative of highly degraded OM (Schellekens et al., 2009; Buurman and Roscoe, 2011). The lowest abundances of the (poly)aromatic and certain aliphatic compounds (i.e., n-alkenes C17–C22 and C27–C28, n-alkanes C13–C16 and alkan-2-ones C13–C17) are observed among the sediments located close to the shoreline (N1–N2, E3, S5, S23), while the two shallow sites situated between the larger north and south basins (M5–M6) present the lowest abundances for all other organic compounds. To identify the most significant relationships between the different organic compound groups and to more precisely explore their spatial distribution, the results of PCA and cluster analyses are further presented and discussed.

3.2.2 Principal components of OM molecular composition

For the OM molecular composition dataset, six principal components (PC1–6_{OM}) were retained, which explain 85 % of the total variance (Fig. 3). PC1$_{OM}$, which captures 30 % of the total variance, separates organic compounds that are produced during OM degradation (positive loadings) from molecules of higher plant or moss origin, including those that are readily mineralized (negative loadings, Fig. 3a). Compounds with positive loadings include (i) (poly)aromatics (i.e., benzene, acetylbenzene, benzaldehyde, alkylbenzenes C2–C9 and polyaromatics) and (ii) degradation products of carbohydrates ((alkyl)furans and furanones; Schellekens et al., 2009), proteins, amino acids, chlorophylls (aromatic N, (alkyl)pyridines and (alkyl)pyrroles; Jokic et al., 2004; Sin-

Table 2. Summary statistics for the molecular composition of sediment OM given as relative abundances (expressed in %) of the 41 groups of pyrolytic organic compounds, which belong to 13 classes of OM as indicated in bold (to be continued).

	Compounds included	$Av^a \pm SD^b$	CV^c	Median	$A:M^d$	Min^e–max^f
Carbohydrates						
(Alkyl)furans & furanones	3-furaldehyde, 2-furaldehyde, 2-acetyl-furan, methyl-3-furaldehyde, 2(5H)-furanone, methyl-2-furaldehyde, dihydro-methyl-furanone, methyl-2(5H)-furanone, methyl-2-furaldehyde	15 ± 4	30	14	1.06	8–28
Hydroxy- or carboxy-furans and furanones	2-furancarboxylic acid, methyl ester; 2,5-dimethyl-4-hydroxy-3(2H)-furanone; 5-(hydroxymethyl)-2-furaldehyde	4.1 ± 1.2	29	4.0	1.03	0.8–7.5
Pyrans	5,6-dihydro-pyran-2-one, 4-hydroxy-5,6-dihydro-pyran-2-one	3.4 ± 1	30	3.2	1.06	1.2–5.3
Dianhydrorhamnose	Dianhydrorhamnose	1.6 ± 0.5	28	1.7	0.99	0.3–2.7
Levoglucosenone	Levoglucosenone	2.2 ± 0.4	20	2.2	1.00	1.3–3.1
Anhydrosugars	Anhydrohexose, levogalactosan, levomannosan, levoglucosan	3.7 ± 2.6	71	2.5	1.46	0.8–11
Chitin-derived compounds						
Chitin-derived compounds	Acetamide, 3-acetamido-furan, 3-acetamido-4-pyrone, oxazoline	2.5 ± 1	40	2.6	0.98	0.2–4.2
N compounds						
(Alkyl)pyridines	Pyridine, 2-methyl-pyridine, 3/4-methyl-pyridine	0.3 ± 0.1	34	0.3	0.95	0.1–0.5
Pyridines_O, i.e., pyridines with side chain containing a "C = O" function	2-acetylpyridine, 3-acetylpyridine, 2-methyl-5-acetoxypyridine	0.7 ± 0.1	18	0.7	1.00	0.2–0.9
(Alkyl)pyrroles	Pyrrole, methyl-pyrrole	2.4 ± 0.5	22	2.4	1.01	1.7–3.5
Pyrroles_O, i.e., pyrroles with side chain containing a "C=O" function	2-formyl-pyrrole, 2-acetyl-pyrrole, 2-formyl-1-methylpyrrole	1.0 ± 0.2	25	0.9	1.04	0.5–1.4
Pyrroledione & pyrrolidinedione	2,5-pyrroledione, 2,5-pyrrolidinedione	1.2 ± 0.3	29	1.2	0.98	0.2–1.7
Aromatic N compounds	Benzeneacetonitrile, benzenepropanenitrile	0.8 ± 0.3	36	0.8	1.03	0.3–1.4
Indoles	Indole, methyl-indole	1.5 ± 0.4	24	1.5	1.03	0.5–3.1
Diketodipyrrole	Diketodipyrrole	0.8 ± 0.2	22	0.8	1.01	0.4–1.2
Diketopiperazines	Pro-Ala, Pro-Val, Pro-Val, Cyclo-Leu-Pro, Pro-Pro, Pro-Phe	1.5 ± 0.4	30	1.5	1.02	0.3–2.6
Alkylamides	Six alkylamides	0.6 ± 0.3	51	0.6	1.06	0.1–1.7

Table 2. Continued.

	Compounds included	Av[a] ± SD[b]	CV[c]	Median	A : M[d]	Min[e]–max[f]
Phenols						
Phenols	Phenol, 2-methyl-phenol, 3/4-methyl-phenol, dimethyl-phenol, ethyl-phenol, propenyl-phenol	8 ± 1	15	8	1.02	4.4–11.4
Lignin						
Syringols	Syringol, 4-vinyl-syringol, 4-formyl-syringol, 4-allenesyringol, acetosyringone	0.5 ± 0.4	83	0.4	1.32	0.1–1.9
Guaiacols	Guaiacol, ethyl-guaiacol, 4-vinyl-guaiacol, 4-propenyl-guaiacol, vanillin, 4-alleneguaiacol, acetovanillone, methyl-ester-vanillic acid, guaiacylacetone	3.6 ± 2.3	65	2.9	1.24	1.1–13.5
Chlorophylls						
Pristenes	Prist-1-ene, prist-2-ene	2.7 ± 0.8	28	2.8	0.97	0.4–4.6
Phytadienes	Phytadiene 1, phytadiene 2	1.9 ± 0.7	35	1.8	1.04	0.2–3.6
n-alkenes						
C9–C16 : 1	n-alkenes C9, C13, C14, C16	3.5 ± 0.8	23	3.6	0.98	1.8–5.1
C17–C22 : 1	n-alkenes C17, C18, C19, C20, C21, C22	6 ± 1	17	6.2	0.97	3.5–8.9
C23–26_1	n-alkenes C23, C24, C25, C26	2.9 ± 0.9	32	2.7	1.09	0.6–5.4
C27–28 : 1	n-alkenes C27, C28	0.8 ± 0.4	47	0.7	1.10	0.1–1.4
n-alkanes						
C10–C16 : 0	n-alkanes C10, C11, C12, C13, C14, C15, C16	2.5 ± 0.6	23	2.5	1.03	1.3–4.1
C17–C22 : 0	n-alkanes C17, C18, C19, C20, C21, C22	3.9 ± 0.8	21	4.0	0.98	1.6–5.4
C23–C26 : 0	n-alkanes C23, C24, C25, C26	2.8 ± 1.4	49	2.7	1.07	1.4–8.8
C27–C35 : 0	n-alkanes C27, C28, C29, C30, C31, C32, C33, C35	4.3 ± 3.5	80	3.6	1.20	1.1–21.3
Alkan-2-ones						
2K C13-17	Alkan-2-ones C13, 16, 17	1.3 ± 0.4	33	1.4	0.96	0.6–2.2
2K C19-21	Alkan-2-ones C19, 20, 21	0.3 ± 0.1	45	0.3	0.97	0–0.8
2K C23-31	Alkan-2-ones C23, 14, 25, 26, 27, 28, 29, 31	1.3 ± 0.8	62	1.1	1.24	0.1–3.3
Steroids						
Steroids	Cholest-2-ene, cholesta-3,5-diene, stigmasta-5,22-dien-3-ol, acetate, sitosterol, cholesta-3,5-dien-7-one, stigmasta-3,5-dien-7-one	1.2 ± 0.9	70	1.1	1.10	0–4.3
Tocopherols						
Tocopherols	γ−tocopherol, α-tocopherol	0.3 ± 0.3	106	0.2	1.75	0–1.5

Table 2. Continued.

	Compounds included	Av[a] ± SD[b]	CV[c]	Median	A : M[d]	Min[e]–max[f]
Hopanoids						
Hopanoids	Trinosphopane, norhopene, 22,29,30-trisnorhop-17(21)-ene, 22,29,30-trisnorhop-16(17)-ene, norhopane, 25-norhopene	1.3 ± 0.4	31	1.4	0.94	0.2–1.9
(Poly)aromatics						
Benzene	Benzene	0.9 ± 0.4	43	0.8	1.14	0.4–2.5
Benzaldehyde	Benzaldehyde	0.6 ± 0.3	41	0.6	1.08	0.3–1.5
Acetylbenzene	Acetyl-benzene	1.1 ± 0.4	39	1.0	1.10	0.6–2.3
Alkylbenzenes C3-9	Ethyl-methyl-benzene, benzene C7, benzene C9,	1.9 ± 0.5	23	1.8	1.07	1.4–3.5
Polyaromatics	Styrene, indene, dihydro-naphthalene, dihydro-inden-1-one, 1-methyl-napthalene, 2-methyl-napthalene, biphenyl, fluorene, anthracene	1.4 ± 0.4	27	1.3	1.04	0.8–2.1

[a] Av.: average. [b] SD: standard deviation. [c] CV: coefficient of variation calculated as relative standard deviation given as a percentage. [d] A : M: ratio between average and median. [e] Min.: minimal value. [f] Max.: maximal value.

ninghe Damsté et al., 1992) and lipids (short-chain n-alkanes – C13–C16 : 0, n-alkenes – C9–C16 : 1 and alkan-2-ones – 2K C13-17; Schellekens et al., 2009). Therefore, positive PC1$_{OM}$ scores represent samples rich in degraded OM. The molecules of plant origin with negative PC1$_{OM}$ loadings are syringol and guaiacol lignin oligomers that are specific for vascular plant, long-chain n-alkenes (C23–C26 : 1 and C27–C28 : 1) derived from lipids of higher plants and/or mosses (Meyers and Ishiwatari, 1993), and long-chain alkan-2-ones (2K C23–C31). Although alkan-2-ones C23–C31 may arise with degradative oxidation of n-alkanes and/or n-alkenes (Zheng et al., 2011), they are also good biomarkers for mosses such as *Sphagnum* (2K C23–C25) and for aquatic higher plants (2K C27–C31) (Baas et al., 2000; Hernandez et al., 2001; Nichols and Huang, 2007). Furthermore, negative loadings on PC1$_{OM}$ are found for the anhydrosugars, which are pyrolytic products of fresh, high-molecular-weight carbohydrates and cellulose from higher plants and mosses (never reported in pyrolysis chromatograms of algae or arthropods; Marbot, 1997; Nguyen et al., 2003; Valdes et al., 2013), as well as for the ratio anhydrosugars: (alkyl)furans and furanones, which are a proxy for plant OM freshness (Fig. 3a; Schellekens et al., 2009). Thus, negative PC1$_{OM}$ loadings likely reflect a fresh pool of OM coming from in-lake vegetation.

PC2$_{OM}$ captures 14 % of the total variance, and positive loadings are associated with (i) mid-chain n-alkanes and/or n-alkene doublets that are known to be released during pyrolysis of resistant biomacromolecules such as cutin, suberin and algaenan (Buurman and Roscoe, 2011); (ii) pristenes,

which are resistant degradation products of chlorophylls (Nguyen et al., 2003); and (iii) hopanoids, which are high-molecular-weight pentacyclic compounds of prokaryotic, especially bacterial, origin (Meredith et al., 2008; Sessions et al., 2013). No compounds are significantly negatively correlated to PC2$_{OM}$ (Fig. 3a). High PC2$_{OM}$ scores thus represent samples rich in organic molecules that are resistant to degradation.

PC3$_{OM}$ explains 13 % of the total variance and separates carbohydrates and N compounds that are pyrolytic or degradation products of proteins, amino acids and/or chlorophylls (i.e., pyridines, pyrroledione and pyrrolidinedione) and of chitin on the positive side, from aliphatic long-chain n-alkanes (C23–C26 : 0 and C27–C35 : 0) from lipids of higher plants or mosses on the negative side (Fig. 3b).

On PC4$_{OM}$, which explains 13 % of the total variance, positive loadings are found for the diketopiperazines, i.e., specific pyrolytic products of proteins or amino acids (Fabbri et al., 2012), the alkylamides and the chlorophyll-derived phytadienes, which altogether indicate fresh algal organic residues (Peulvé et al., 1996; Nguyen et al., 2003; Fabbri et al., 2005; Micić et al., 2010). Pyrolytic products of chitin (Gupta et al., 2007) and hopanoids, which derive from prokaryotes and mainly bacteria (Meredith et al., 2008; Sessions et al., 2013), also have positive loadings on PC4$_{OM}$, while no compounds are significantly negatively correlated to PC4$_{OM}$ (Fig. 3b). Therefore, PC4$_{OM}$ reflects OM input from in-lake algae and microorganisms (e.g., zooplankton, bacteria). Steroids, which have not yet been reported by Py–GC–MS in aquatic matrices, have positive loadings on this

Table 3. Whole-lake and cluster averages for a selection of elemental geochemical parameters and of ratios indicative of OM source types and their degradation status.

Specific features in geochemistry

	Whole-lake[a]	Near-shore sites	North-east basins	Shallower–intermediate depth	Intermediate depth	Deeper	Shallow central areas
		Clustergeo 4	Clustergeo 1	Clustergeo 6	Clustergeo 2	Clustergeo 5	Clustergeo 3
	$(n^b=42)$	$(n=4)$	$(n=13)$	$(n=10)$	$(n=8)$	$(n=3)$	$(n=4)$
Water depth (m)	9±7 (78 %)[c]	4±2	5±3	8±3	15±4	24±1	2±1
Bulk density (g cm^{-3})	0.06±0.02 (33 %)	0.06±0.03	0.07±0.02	0.07±0.02	0.05±0.01	0.026±0.009	0.10±0.02
[bSi] (%)	13±6 (46 %)	12±6	13±3	15±7	15±4	4.2±0.3	21±4
[LOI] (%)	38±10 (26 %)	50±12	39±5	34±7	37±4	52±2	20±8
[S] (mg kg^{-1})	11 876±5920 (50 %)	17 510±833	11 683±3440	7550±1900	12 896±3315	26 227±4833	4879±148
[Br] (mg kg^{-1})	149±35 (23 %)	130±6	153±36	145±35	154±19	204±26	116±32
[Cu] (mg kg^{-1})	34±13 (38 %)	36±5	28±6	30±7	42±6	65±10	24±13
[Ni] (mg kg^{-1})	19±5 (25 %)	21±1	18±4	17±2	21±4	27±1	12±4
[Hg] (µg kg^{-1})	337±202 (60 %)	407±141	251±47	230±69	427±94	917±212	203±87
[Zn] (µg kg^{-1})	219±108 (49 %)	279±31	212±68	139±42	305±86	417±33	63±16
[Fe] (%)	5±3 (60 %)	3.1±2.1	2.7±1.7	3.6±1.5	9.1±2.4	4.3±2.2	5.5±1.7
Fe : Al	1.5±0.8 (53 %)	1.0±0.5	1.0±0.6	1.1±0.3	2.5±0.9	1.3±0.6	1.9±0.3
[As] (mg kg^{-1})	35±20 (57 %)	27±17	26±16	25±11	64±11	48±14	29±9
[P] (mg kg^{-1})	1624±741 (46 %)	927±240	1065±295	2088±730	2074±275	2766±869	1224±216
[Mn] (mg kg^{-1})	729±1690 (231 %)	162±53	182±67	184±50	305±93	171±13	5700±1597
Mn : Fe	0.02±0.03 (150 %)	0.007±0.002	0.008±0.003	0.006±0.002	0.004±0.001	0.005±0.002	0.111±0.051
[Co] (mg kg^{-1})	19±15 (79 %)	15±8	12±6	13±5	26±11	14±2	49±24
[Pb] (mg kg^{-1})	192±90 (47 %)	199±58	132±53	115±42	300±59	315±7	182±96

Specific features in OM composition

		Whole-lake	Near-shore sites	North-east basins	South basin			Shallow central areas
			ClusterOM 5	ClusterOM 1	ClusterOM 3	ClusterOM 2	ClusterOM 4	ClusterOM 6
		$(n=42)$	$(n=4)$	$(n=16)$	$(n=14)$	$(n=3)$	$(n=3)$	$(n=2)$
Water depth (W.D.) (m)		9±7 (78 %)	4±2	7±5	11±5	24.1±0.5	3.2±0.9	1.8±0.1
LOI (%)		38±10 (26 %)	50±12	39±4	36±5	52±2	24±4	14±6
(C23–C35 : 0+2K C23–C31) : lignin[d]	In-lake : terrestrial plant OM	2±1 (50 %)	0.8±0.5	3±1	1.7±0.4	1.8±0.6	3±1	19±11
N compounds : carbohydrates	Algal : plant OM[d]	0.37±0.09 (24 %)	0.32±0.08	0.35±0.04	0.39±0.05	0.6±0.1	0.29±0.02	0.23±0.05
Chlorophylls : plant lipids+lignin[d]	Algal : plant OM	0.18±0.09 (50 %)	0.10±0.05	0.13±0.06	0.24±0.08	0.31±0.07	0.18±0.05	0.03±0.03
Proteins : (alkyl)pyrroles+(alkyl)pyridines+aromatic N[d]	Algal OM (N compounds) freshness	0.3±0.1 (33 %)	0.39±0.09	0.36±0.05	0.22±0.06	0.42±0.06	0.20±0.08	0.13±0.08
Phytadienes : pristenes[d]	Algal OM (chlorophylls) freshness	0.4±0.1 (25 %)	0.4±0.1	0.37±0.09	0.40±0.06	0.56±0.05	0.42±0.07	0.5±0.2
Anhydrosugars : (alkyl)furans & furanones[d]	Plant OM (carbohydrates) freshness	0.2±0.2 (100 %)	0.4±0.2	0.3±0.2	0.12±0.11	0.14±0.04	0.08±0.01	0.042±0.002
Guaiacyl-acid : guaiacyl-1C[d]	Plant OM (lignin) freshness	0.07±0.03 (43 %)	0.13±0.02	0.07±0.03	0.05±0.02	0.04±0.01	0.04±0.03	0.10±0.06
Guaiacyl-2C : guaiacyl-1C[d]	Plant OM (lignin) freshness	0.8±0.3 (38 %)	1.23±0.07	1.0±0.2	0.5±0.2	0.6±0.2	0.5±0.1	1.1±0.2
Syringyl-2C : syringyl-1C[d]	Plant OM (lignin) freshness	1.0±0.8 (80 %)	2.4±0.3	1.1±0.6	0.5±0.2	0.6±0.1	0.3±0.3	1.4±0.8

[a] Whole-lake: averages of all analyzed sediment samples excluding the two outlier samples (sites M4, S15; see Sect. 3.1.1). [b] n: number of samples. [c] The data are presented as follows: average ± SD (relative standard deviation). [d] The compounds included in the ratios are given in detail in Tables 2 and S1; italic font denotes average values below the whole-lake average (< 10 %); normal font denotes values close to the whole-lake average (±10 %); bold font denotes values above the whole-lake average (> 10 %).
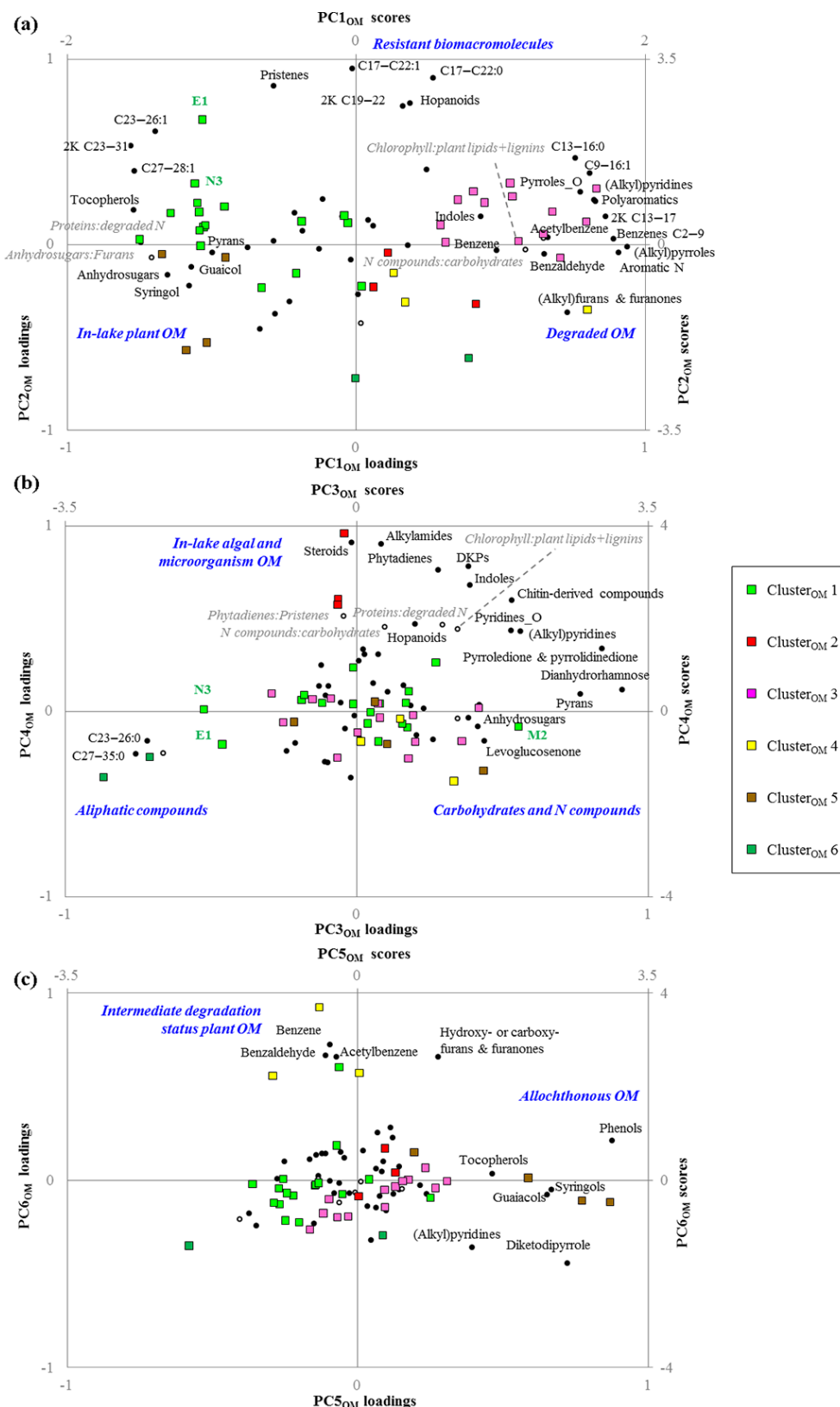
Figure 3. Combined loading and score plots for PCs 1–6 **(a–c)** of the OM molecular composition dataset (i.e., the 41 groups of organic compounds as defined in Table 2). For the PC loadings, filled circles correspond to active variables. Other variables (empty circle and italics) were added passively. Sediment samples are colored according to the results of the cluster analysis.

PC4$_{OM}$, suggesting that the steroids released by pyrolysis in aquatic samples are mainly of algal origin.

For PC5$_{OM}$, capturing 8 % of the total variance, positive loadings are related to lignin oligomers, which are specific for vascular plants (Meyers and Ishiwatari, 1993), and diketodipyrrole, a N compound often reported in soil pyrolysates (e.g., Schellekens et al., 2009; Buurman and Roscoe, 2011). No compounds are associated with negative loadings on PC5$_{OM}$ (Fig. 3c). Interestingly, the long-chain n-alkanes from higher plants or moss lipids do not have positive loadings on PC5$_{OM}$. We therefore interpret PC5$_{OM}$ to relate to OM inputs from the forested catchment, which is dominated by coniferous species. Coniferous trees generally have higher lignin contents as compared to other vascular plants (Campbell and Sederof, 1996), while they contain much lower amounts of n-alkanes than other plant species (Bush and McInerney, 2013).

PC6$_{OM}$ captures 7 % of the total variance and has four compounds with significant positive loadings, i.e., benzene, two benzenes with oxidized side-chain and carboxy- or hydroxy-furans, and furanones, i.e., furan and furanone heterocycles with an O atom in the side-chain (Fig. 3c). PC6$_{OM}$ may thus represent an intermediate degradation status of higher plant and/or moss residues between the lignin oligomers or anhydrosugars (fresh) and the degraded polyaromatics and benzenes C2–C9 or (alkyl)furans and furanones (i.e., furan and furanone heterocycles with an aliphatic side chain).

3.2.3 Cluster analysis of OM composition

As with the elemental geochemistry dataset, a solution of six clusters (cluster$_{OM}$ 1–6) was relevant to represent the data on the spatial heterogeneity of OM molecular composition (Fig. 1d). Each cluster is associated with one or a few of the OM types that were identified by the PC1–6$_{OM}$ (Fig. 3; Sect. 3.2.1). The cluster averages and standard deviations of each organic compound are given and compared to whole-lake averages in Table S5. Table 3 provides the cluster averages for ratios indicative of OM source types and their degradation status based on literature data and on the distribution of the organic compounds on PC1–6$_{OM}$.

In the south basin, the majority of sites found at shallower and intermediate water depths group in cluster$_{OM}$ 3 ($n = 14$) and are enriched in degraded and resistant OM (positive scores on PC1$_{OM}$, Fig. 3a). The deep basin sites (cluster$_{OM}$ 2, $n = 3$) are enriched in fresh algal and zooplanktonic OM (positive scores on PC4$_{OM}$, Fig. 3b). Accordingly, the values for the ratios indicative of higher proportions of fresh, labile algal OM, based on N-compound or chlorophyll composition, are higher in the deeper sites as compared to whole-lake averages, while the values are below or within ±10 % of whole-lake averages in the sediments found at shallower and intermediate water depths (Table 1). In contrast, the ratios indicative of higher plant and moss OM freshness based on

carbohydrate or lignin composition have similar values and are lower as compared to whole-lake averages for all sediments of the south basin. Furthermore, the clusters$_{OM}$ 2 and 3 are characterized by higher values for the ratios specific of algal versus higher plant and moss OM based on the proportions of N compounds versus carbohydrates or chlorophylls versus lignin and long-chain n-alkanes and alkan-2-ones (Table 1). The rest of the south basin sites fall within cluster$_{OM}$ 1 ($n = 1$), 5 ($n = 2$) or 4 ($n = 1$), which are described below.

The majority of sites in the northern half of the lake group within cluster$_{OM}$ 1 ($n = 15$), with isolated shallower sites falling within clusters$_{OM}$ 3 ($n = 1$), 4 ($n = 2$) and 5 ($n = 2$). The sediments of cluster$_{OM}$ 1 are rich in fresh plant (higher plants or mosses) OM coming from in-lake productivity (negative scores on PC1$_{OM}$; Fig. 3a) and have higher values than whole-lake averages for the ratios specific of in-lake vs. terrestrial plant OM and of higher plant OM freshness (Table 1). In contrast, the values for these ratios are below 10 % of whole-lake averages for the south basin sites, indicating that terrestrial input is the main source of plant OM to the sediments of the main basin of Härsvatten.

The cluster$_{OM}$ 5 represents some near-shore locations ($n = 4$), which are enriched in OM derived from the coniferous-forested catchment (positive scores on PC5$_{OM}$, Fig. 3c). The cluster$_{OM}$ 4 ($n = 4$), which groups shallow sites located close to the lake outlet (south basin, S16) and between the north and east basins (N10 and M1), is characterized by high proportions of degraded and resistant OM (positive scores on PC5$_{OM}$, Fig. 3a). Two shallow sites of the central area (cluster$_{OM}$ 6, $n = 2$) show an enrichment in aliphatic molecules derived from higher plant and moss lipids (negative loadings on PC3$_{OM}$; Fig. 3b). Both clusters$_{OM}$ 4 and 6 have values for the ratio indicative of in-lake : terrestrial plant OM above 10 % of the whole-lake average, while the values for the ratios specific of algal vs. higher plant and moss OM and of OM freshness based on N-compound and carbohydrate composition are below 10 % of whole-lake averages (Table 1). Cluster$_{OM}$ 6 differs from cluster$_{OM}$ 4 by its higher values for the ratios specific of OM freshness based on chlorophyll and lignin composition.

3.3 Factors and processes involved in the spatial distribution of OM molecular composition

The surface sediments used in this study comprise the uppermost 10 cm. Given the inherent variation in sedimentation rates across a lake basin, each bulk sample represents material deposited over different timescales. We know from the developmental work for our Py–GC–MS method using annually laminated sediments that there are transformations in OM composition within the uppermost few centimeters, i.e., the first few years following deposition (Tolu et al., 2015). Thus, these bulk sediment samples provide initial insights into the spatial variability in molecular OM composition within a lake basin resulting from longer-term sedi-

mentation processes (including those within the sediment), reflecting years to decades.

The distribution of both clusters$_{geo}$ and clusters$_{OM}$ within Härsvatten shows a similar general pattern (Fig. 1c and d), where a main feature is the separation of most of the sediments located in the north and east basins (cluster$_{geo}$ 1 and cluster$_{OM}$ 1) from those found in the main south basin (clusters$_{geo}$ 2, 5, and 6 and clusters$_{OM}$ 2 and 3). The other similarities are (i) a separation of the sediments within the main, south basin according to water depth, with cluster$_{geo}$ 5 and cluster$_{OM}$ 2 grouping the deeper sites and clusters$_{geo}$ 2 and 6 and cluster$_{OM}$ 3 grouping the shallow and intermediate depth sites; and (ii) a separation of the shallower sites that are located close to the shore (cluster$_{geo}$ 4 and cluster$_{OM}$ 5) from the ones found between the north and east basins and between the central area and the south basins (cluster$_{geo}$ 3 and clusters$_{OM}$ 4 and 6).

3.3.1 Spatial variability in the main south basin

As shown previously for OM (as % LOI) and Pb (Bindler et al. 2001), there is a physical and inorganic geochemical gradient from shallower to deeper waters reflecting sediment focusing in the south basin of Härsvatten. B.D. and bSi decrease from shallower (cluster$_{geo}$6) to intermediate (cluster$_{geo}$2) and to deeper areas (cluster$_{geo}$5), whereas there is a progressive enrichment in organic matter and trace elements with increasing water depth (Fig. 1c; Table 1). For example, B.D. decreases from ~ 0.07 to 0.03 g cm^{-3}, while OM and Hg increase from ~ 34 to 52% and from ~ 230 to 920 ng g^{-1}, respectively, in shallower versus the deepest locations. At intermediate depths (cluster$_{geo}$2), OM, B.D., bSi and most trace metals (i.e., Cu, Ni, Hg, Zn) are between those of shallow and deep locations. Sediment focusing is thus an important process for sediment geochemistry in the large, deep basin of Härsvatten, which presents a relatively simple morphometry. According to the model of sediment focusing, the sediments found at shallower (< 11 m, cluster$_{geo}$ 6), intermediate ($11–21$ m, cluster$_{geo}$ 4) and deeper water depths (> 23 m, cluster$_{geo}$ 5) would correspond to zones of erosion, transportation and accumulation, respectively (Håkanson, 1977). The bSi decline, from ~ 15 to 4%, indicates a decrease of diatom production with depth due to increasing light attenuation and thus suggests that the diatom assemblage is dominated by benthic diatoms, as shown for many acidified lakes, such as the surrounding lakes in the Svartedalen nature reserve (e.g., Andersson, 1985; Anderson and Renberg, 1992).

In this main basin of Härsvatten, OM originates from a combination of autochthonous algal production and allochthonous input (Sect. 3.2.2). The dominance of benthic diatoms in acidified lakes and the declining bSi content with depth would indicate that the algal material in deeper areas of the basin should mainly derive from resuspended benthic algal production. However, this benthic algal pro-

duction is not reflected in the OM molecular composition. The sediments from shallow and intermediate water depths (cluster$_{OM}$ 3) are mainly composed of degraded and resistant OM, while the sediments from deeper sites (cluster$_{OM}$ 2) are enriched in fresh algal and zooplanktonic OM (Fig. 1d; Sect. 3.2.2). Although our results are based on the top 10 cm of sediment and thus account for different sediment ages, we suggest that the higher proportions of decomposed algal material, based on N-compound and chlorophyll composition (Table 1), at shallower and intermediate water depths (< 21 m) than at the deepest sites ($23.5–24.5$ m) reflect higher mineralization rates of OM in shallow–intermediate areas. Higher OM mineralization rates in shallow–intermediate areas are most probably due to more oxic conditions, which are known to prevail in epilimnetic and metalimnetic sediments (Ostovsky and Yacobi, 1999); the epilimnion in Härsvatten has been assessed to extend to 10–15 m water depth. Higher OM preservation in the deeper area may also be favored by higher accumulation rates as compared to shallow–intermediate areas (as a consequence of sediment focusing), but the sedimentation rates in the deeper areas of Härsvatten are nonetheless very low, with the uppermost 30 cm being deposited during the last ca. 500 years (Bindler et al., 2001). Moreover, the elemental geochemistry indicates that the sites found at intermediate water depths (cluster$_{geo}$ 6, 11–21 m) correspond in the sediment focusing model to transportation zones, which experience recurrent resuspension events that favor gas exchanges and mineralization of OM (Ståhlberg et al., 2006). Occurrence of oxic conditions at intermediate depths in the south basin is supported by the higher concentrations of Fe, Mn, As, Co and P and the high Fe : Al values, this combination of parameters being often indicative of Fe and Mn (oxy)hydroxides (Table 1; Sect. 3.1.1). In line with our hypothesis, higher OM mineralization rates in oxic versus anoxic sediments have previously been reported (Bastviken et al., 2004; Isidorova et al., 2016). However, in contrast to the more algal-derived OM, we do not observe significant differences between the sediments of shallower–intermediate water depths and the deepest sites for ratios indicative of higher plant and moss OM freshness (Table 1). Because higher plant and moss OM is mainly of allochthonous origin in this basin, our results indicate that primarily autochthonous algal OM is mineralized in the epilimnetic and metalimnetic sediments of this deeper, steeper-sloped basin of Härsvatten. This is consistent with the suggestion that allochthonous OM is recalcitrant to sediment mineralization after its degradation in the catchment and within the water column (Gudasz et al., 2012).

Overall, our molecular characterization of OM in the south basin suggests an enrichment in algal versus allochthonous OM (e.g., higher N compound : carbohydrate ratio) in the deeper areas of a deep, simple lake basin, in line with previously reported sediment C : N ratios along lake-basin transects (Kumke et al., 2005; Dunn et al., 2008; Bruesewitz et al., 2012). Given our data on the degradation status of al-

gal and allochthonous OM, we believe that this trend in OM quality results from preferential degradation of algal versus allochthonous OM in sediments at shallower–intermediate water depth in addition to the known focusing of living, and residues of, autochthonous OM towards deeper sites (Ostrovsky and Yacobi, 1999).

3.3.2 Spatial variability in the central, north and east basins and near-shore locations

In the northern half of the lake, 11 of 19 locations fall within cluster$_{geo}$1 (Fig. 1c), which only distinguishes itself geochemically by somewhat-lower-than-average concentrations of elements often associated with (oxy)hydroxides (i.e., Fe, Mn, As, P and Co; Table 1 and Sect. 3.1.2). Sediments from the shallowest locations can potentially fall into one of four different clusters (clusters$_{geo}$ 1, 3, 4 or 6). Thus, for the northern half of the lake there is no evidence of sediment focusing. The effect is either limited by the more gentle slopes of the north and east basins (Blais and Kalff, 1995), modified by the water circulation resulting from the prevailing winds towards the northeast (Bindler et al., 2001; Abril et al., 2004), and/or interrupted by aquatic vegetation that acts as a sediment trap (Benoy and Kalff, 1999). Aquatic vegetation represents a major source of OM to the sediments of the north, east and central basins (clusters$_{OM}$ 1, 4 and 6; Fig. 1d; Table 1; Sect. 3.2.2). The enrichment of aquatic higher plant or moss OM in these sediments is consistent with field observations during the original sediment coring in winter 1997, where mosses and *Isoetes* (a vascular angiosperm plant) were observed in some parts of the lake to a depth of at least 10 m (Bindler et al., 2001). The presence of such submerged vegetation in Härsvatten is favored by its clear acidic water (i.e., deeper light penetration), as previously observed for other acidified boreal Swedish lakes, such as the nearby lake Gårdsjön (Andersson, 1985; Grahn, 1985). Benthic aquatic vegetation is also favored in the northern half of Härsvatten by the more gentle slopes, with comparatively shallow water depth and thus greater availability of light than in the deep, steeper-sloped south basin where allochthonous input appears as the main source of higher plant and moss OM (Sect. 3.2.2; Table 1).

The sediments found across the north and east basins and at the deeper sampling site of the central area (clusters$_{OM}$ 1, Fig. 1d) have the highest proportions of fresh, labile higher plant and moss OM, e.g., anhydrosugars (Sect. 3.2.2, Table 1). Also, the proportions of fresh, labile algal OM are as high as in the deeper anoxic sediments of the main south basin and 2 times higher than in the sediments found at shallow water depth in the south basin and central areas, although these sites span the same water depth range (3–11 m) and have relatively similar bSi contents (Table 1). These results indicate the accumulation of fresh autochthonous, both plant and algal, OM in sediments associated with in-lake vegetation even if they are below or within the epilimnion (i.e., sup-

posed oxic conditions). A possible explanation is that the input of labile, decomposing in-lake higher plant and moss OM consumes oxygen and results in locally anoxic conditions in the sediment, which in turn lower OM mineralization rates (Bastviken et al., 2004; Isidorova et al., 2016). This hypothesis may explain the lower-than-whole-lake-average concentrations of elements or elemental ratios often associated with (oxy)hydroxides (i.e., Fe, Mn, As, Co, P contents and Fe : Al) in these epilimnetic–metalimnetic sediments (cluster$_{geo}$ 1, Table 1). This interpretation is consistent with laboratory experiments, where, for example, Kleeberg (2013) had shown that inputs of macrophyte residues to sediments result in oxygen depletion and microbially mediated reduction of Fe and Mn oxides. However, we cannot rule out that other factors, such as shallow groundwater discharges that are rich in (oxy)hydroxides or diagenetic processes that lead to Fe enrichment in sediments, can be involved in the higher concentrations of Fe, Mn and other elements known to be associated with Fe and Mn (oxy)hydroxides in the sediments of the south basin as compared to the sediments of the north and south basins.

The shallow sites located between the north and east basins and between the central area and the south basin (i.e., cluster$_{geo}$ 3 and clusters$_{OM}$ 4 and 6; Fig. 1c and d) have higher-than-whole-lake-average bSi contents and values for the ratio of in-lake : terrestrial higher plant and moss OM, suggesting that these sediments receive plant OM from in-lake vegetation and algal OM from benthic production (Table 1). However, the proportions of fresh, labile plant and algal OM based on N-compound and carbohydrate composition in these central sediments are much lower than in the sediments found across the north and east basins (Table 1). These central areas are probably not sites for aquatic vegetation growth, but they receive in-lake plant OM produced within the north and east basins that has been degraded during transport and/or is degraded at these shallow central sites due to more oxic conditions. More oxic conditions at these shallow central sites are also suggested by a higher occurrence of Fe and Mn (oxy)hydroxides (Fe, Mn, As, Co, and P contents, Fe : Al and Mn : Fe above 10 % of whole-lake averages; Table 1). Among these shallow central sites, two locations (cluster$_{OM}$ 6) are specifically rich in higher plant and moss lipids (i.e., C23–C35 : 0; Table S3) and have high proportions of fresh higher plant OM based on lignin composition, while the proportions of fresh carbohydrates (anhydrosugars) versus total carbohydrates is low (Table 1). This suggests preservation of higher plant cell-wall lipids and lignin with respect to carbohydrates at these two shallow sites, in agreement with the known faster assimilation of carbohydrates versus lipid and lignin structures (Bianchi and Canuel, 2011). However, no reasonable hypothesis could be given to explain this difference in OM molecular composition between the sediments at sites M5–M6 and the ones at sites N10 and M1 given their similar water depth and elemental geochemistry.

Among the sediments found in a small number of near-shore locations (cluster$_{geo}$ 4 and cluster$_{OM}$ 5, $n = 4$), three are located in two more-sheltered bays at the northwestern corner and the southern end of the lake that are more protected from wind circulation (Bindler et al., 2001; Abril et al., 2004). The sediments of these three locations predominantly accumulate terrestrial OM, as indicated by the abundance in lignin oligomers and the ratio indicative of in-lake : terrestrial plant OM that are respectively above and below 10 % of the whole-lake averages (Table 3). Accumulation of OM coming from the coniferous-forested catchment most probably explained the high OM content (i.e., 52–58 %, which is as high as in the deeper sediments of the main south basin) as well as the high concentrations of S and trace metals (i.e., Hg, Pb and Zn) in these near-shore sediments (Table 1). Boreal forest soils are known to be enriched in S and trace metals because their organic fraction retains atmospheric S and trace metals deposited over the industrial era (Johansson and Tyler, 2001). Also, there is evidence that the transport of terrestrial OM to boreal aquatic ecosystems is associated with significant inputs of trace metals (Grigal, 2002; Rydberg et al., 2008). Alternatively, high S and trace metal contents could be due to accumulation of metal sulfides due to near-shore groundwater gradients and/or anoxic conditions, or to redox cycling related to the important input of terrestrial OM.

3.3.3 Implication for in-lake and/or global elemental (e.g., C, nutrients, trace metals) cycling

The molecular composition of natural OM has been shown to exert a strong influence on key biogeochemical reactions involved in in-lake and global cycling of C, nutrients and trace metals, such as C mineralization or nutrients–trace metal sorption and transformations into mobile and/or bioavailable species (Drott A et al., 2007; Sobek et al., 2011; Gudasz et al., 2012; Tjerngren et al., 2012; Kleeberg, 2013; Bravo et al., 2017). Our work demonstrates that OM molecular composition can vary significantly within a single lake system in relation to basin morphometry, lake chemical and biological status (e.g., presence of macrophytes, which is influenced by, acidification, for example) and the molecular structure and properties of the different OM compounds (e.g., higher resistance of allochthonous versus autochthonous OM upon degradation). Our results further show that it may be problematic to extrapolate data on OM composition from only a few sites or one basin when scaling up to a whole lake. Thus, investigating sedimentary processes and the resulting fate of C and trace elements using sampling strategies focused on the deepest area of a lake or on single transects from shallower to deeper sites, may not fully capture the variation in either elemental geochemistry or OM composition.

Overall, this study underlines that the OM molecular composition and its spatial heterogeneity across a lake are two factors that should be considered to better constrain processes involved in the fate of C, nutrients and trace metals in lake ecosystems to improve whole-lake budgets for these elements and to better assess pollution risks and the role of lakes in global elemental cycles.

The Supplement related to this article is available online at doi:10.5194/bg-14-1773-2017-supplement.

Author contributions. Julie Tolu and Richard Bindler designed the research. Julie Tolu performed Py–GC–MS analyses with help from Lorenz Gerber and did the data treatment with the data processing pipeline of Lorenz Gerber. Julie Tolu and Johan Rydberg performed XRF and mercury analyses. Julie Tolu and Carsten Meyer-Jacob performed FTIR measurements and Carsten Meyer-Jacob determined the inferred bSi. Julie Tolu, Johan Rydberg, Carsten Meyer-Jacob and Richard Bindler interpreted the data. Julie Tolu prepared the manuscript with consistent contributions from Johan Rydberg, Richard Bindler and Carsten Meyer-Jacob.

References

Abril, J. M., El-Mrabet, R., and Barros, H.: The importance of recording physical and chemical variables simultaneously with remote radiological surveillance of aquatic systems: a perspective for environmental modelling, J. Environ. Radioactiv., 72, 145–152, 2004.

Amon, R. M. W. and Fitznar, H. P.: Linkages among the bioreactivity, chemical composition, and diagenetic state of marine dissolved organic matter, Limnol. Oceanogr., 46, 287–297, 2001.

Anderson, N. J. and Renberg, I.: A palaeolimnological assessment of diatom production responses to lake acidification, Environ. Pollut., 78, 113–119, 1992.

Andersson, B. I.: Properties and chemical composition of surficial sediments in the acidified Lake Gårdsjön, SW Sweden., Ecol. Bull., 37, 251–262, 1985.

Baas, M., Pancost, R., Van Geel, B., and Sinninghe Damsté, J. S.: A comparative study of lipids in Sphagnum species, Org. Geochem., 31, 535–541, 2000.

Ball, D. F.: Loss-on-ignition as estimate of organic matter and organic carbon in non-calcareous soils, J. Soil Sci., 15, 84–92, 1964.

Bastviken, D., Persson, L., Odham, G., and Tranvik, L.: Degradation of dissolved organic matter in oxic and anoxic lake water, Limnol. Oceanogr., 49, 109–116, 2004.

Benoy, G. A. and Kalff, J.: Sediment accumulation and Pb burdens in submerged macrophyte beds, Limnol. Oceanogr., 44, 1081–1090, 1999.

Bianchi, T. S. and Canuel, E. A.: Chapter 2: Chemical biomarkers application to ecology and paleoecology, in: Chemical biomarkers in aquatic ecosystems, Princeton University press, Princeton (New Jersey, USA), 19–29, 2011.

Bindler, R., Renberg, I., Brannvall, M. L., Emteryd, O., and El-Daoushy, F.: A whole-basin study of sediment accumulation using stable lead isotopes and flyash particles in an acidified lake, Sweden, Limnol. Oceanogr., 46, 178–188, 2001.

Blais, J. M. and Kalff, J.: The influence of lake morphometry on sediment focusing, Limnol. Oceanogr., 40, 582–588, 1995.

Bravo, A. G., Bouchet, S., Tolu, J., Björn, E., Mateos-Rivera, A., and Bertilsson, S.: Molecular composition of organic matter controls methylmercury formation in boreal lakes, Nat. Commun., 8, 14255, doi:10.1038/ncomms14255, 2017.

Bruesewitz, D. A., Tank, J. L., and Hamilton, S. K.: Incorporating spatial variation of nitrification and denitrification rates into whole-lake nitrogen dynamics, J. Geophys. Res.-Biogeo., 117, G00N07, doi:10.1029/2012JG002006, 2012.

Bush, R. T. and McInerney, F. A.: Leaf wax n-alkane distributions in and across modern plants: Implications for paleoecology and chemotaxonomy, Geochim. Cosmochim. Acta, 117, 161-179, 2013.

Buurman, P. and Roscoe, R.: Different chemical composition of free light, occluded light and extractable SOM fractions in soils of Cerrado and tilled and untilled fields, Minas Gerais, Brazil: A pyrolysis-GC/MS study, Eur. J. Soil Sci., 62, 253–266, 2011.

Buurman, P., Van Bergen, P. F., Jongmans, A. G., Meijer, E. L., Duran, B., and Van Lagen, B.: Spatial and temporal variation in podzol organic matter studied by pyrolysis-gas chromatography/mass spectrometry and micromorphology, Eur. J. Soil Sci., 56, 253–270, 2005.

Campbell, M. M. and Sederof, R. R.: Variation in Lignin Content and Composition, Plant Physiol., 110, 3–13, 1996.

Carr, A. S., Boom, A., Chase, B. M., Roberts, D. L., and Roberts, Z. E.: Molecular fingerprinting of wetland organic matter using pyrolysis-GC/MS: An example from the southern Cape coastline of South Africa, J. Paleolimnol., 44, 947–961, 2010.

Dauwe, B. and Middelburg, J. J.: Amino acids and hexosamines as indicators of organic matter degradation state in North Sea sediments, Limnol. Oceanogr., 43, 782–798, 1998.

De La Rosa, J. M., González-Pérez, J. A., González-Vila, F. J., Knicker, H., and Araújo, M. F.: Molecular composition of sedimentary humic acids from South West Iberian Peninsula: A multi-proxy approach, Org. Geochem., 42, 791–802, 2011.

Drott, A., Lambertsson, L., Bjorn, E., and Skyllberg, U.: Importance of dissolved neutral mercury sulfides for methyl mercury production in contaminated sediments, Environ. Sci. Technol., 41, 2270–2276, 2007.

Dunn, R. J. K., Welsh, D. T., Teasdale, P. R., Lee, S. Y., Lemckert, C. J., and Meziane, T.: Investigating the distribution and sources of organic matter in surface sediment of Coombabah Lake (Australia) using elemental, isotopic and fatty acid biomarkers, Cont. Shelf Res., 28, 2535–2549, 2008.

Fabbri, D., Sangiorgi, F., and Vassura, I.: Pyrolysis-GC-MS to trace terrigenous organic matter in marine sediments: A comparison between pyrolytic and lipid markers in the Adriatic Sea, Anal. Chim. Acta, 530, 253–261, 2005.

Fabbri, D., Adamiano, A., Falini, G., De Marco, R., and Mancini, I.: Analytical pyrolysis of dipeptides containing proline and amino acids with polar side chains, Novel 2,5-diketopiperazine markers in the pyrolysates of proteins, J. Anal. Appl. Pyrolysis, 95, 145–155, 2012

Faix, O., Meier, D., and Fortmann, I.: Thermal degradation products of wood: gas chromatographic separation and mass spectrometric characterization of monomeric lignin derived products, Holz als Roh- und Werkstoff, 48, 281–285, 1990.

Faix, O., Fortmann, I., Bremer, J., and Meier, D.: Thermal degradation products of wood: gas chromatographic separation and mass spectrometric characterization of polysaccharide derived products, Holz als Roh- und Werkstoff, 49, 213–219, 1991.

Fichez, R.: Composition and fate of organic matter in submarine cave sediments; implications for the biogeochemical cycle of organic carbon, Oceanol. Acta, 14, 369–377, 1991.

Grahn, O.: Macrophyte biomass and production in Lake Gårdsjön – an acidified clearwater lake in the SW Sweden, Ecol. Bull., 37, 203–212, 1985.

Grigal, D. F.: Inputs and outputs of mercury from terrestrial watersheds: a review, Environ. Rev., 10, 1–39, 2002.

Gudasz, C., Bastviken, D., Premke, K., Steger, K., and Tranvik, L. J.: Constrained microbial processing of allochthonous organic carbon in boreal lake sediments, Limnol. Oceanogr., 57, 163–175, 2012.

Gupta, N. S., Briggs, D. E. G., Collinson, M. E., Evershed, R. P., Michels, R., and Pancost, R. D.: Molecular preservation of plant and insect cuticles from the Oligocene Enspel Formation, Germany: Evidence against derivation of aliphatic polymer from sediment, Org. Geochem., 38, 404–418, 2007.

Håkanson, L.: The influence of wind, fetch and water depth on the distribution of sediments in Lake Vanern, Sweden, Can. J. Earth Sci., 14, 397–412, 1977.

Hawkes, J. A., Dittmar, T., Patriarca, C., Tranvik, L., and Bergquist, J.: Evaluation of the Orbitrap Mass Spectrometer for the Molecular Fingerprinting Analysis of Natural Dissolved Organic Matter, Anal. Chem., 88, 7698–7704, 2016.

Heathcote, A. J., Anderson, N. J., Prairie, Y. T., Engstrom, D. R., and Del Giorgio, P. A.: Large increases in carbon burial in northern lakes during the Anthropocene, Nat. Commun., 6, doi:10.1038/ncomms10016, 2015.

Hernandez, M. E., Mead, R., Peralba, M. C., and Jaffé, R.: Origin and transport of n-alkane-2-ones in a subtropical estuary: Potential biomarkers for seagrass-derived organic matter, Org. Geochem., 32, 21–32, 2001.

Isidorova, A., Bravo, A. G., Riise, G., Bouchet, S., Bjorn, E., and Sobek, S.: The effect of lake browning and respiration mode on the burial and fate of carbon and mercury in the sediment of two boreal lakes, J. Geophys. Res.-Biogeo., 121, 233–245, 2016.

Johansson, K. and Tyler, G.: Impact of atmospheric long range transport of lead, mercury and cadmium on the Swedish forest environment, Water Air Soil Pollut., 425, 279–297, 2001.

Jokic, A., Schulten, H. R., Cutler, J. N., Schnitzer, M., and Huang, P. M.: A significant abiotic pathway for the formation of unknown nitrogen in nature, Geophys. Res. Lett., 31, L05502, doi:10.1029/2003GL018520, 2004.

Kaal, J., Baldock, J. A., Buurman, P., Nierop, K. G. J., Pontevedra-Pombal, X., and Martínez-Cortizas, A.: Evaluating pyrolysis-GC/MS and ^{13}C CPMAS NMR in conjunction with a molecular mixing model of the Penido Vello peat deposit, NW Spain, Org. Geochem., 38, 1097–1111, 2007.

Kellerman, A. M., Dittmar, T., Kothawala, D. N., and Tranvik, L. J.: Chemodiversity of dissolved organic matter in lakes driven by climate and hydrology, Nat. Commun., 5, 4804, doi:10.1038/ncomms4804, 2014.

Kellerman, A. M., Kothawala, D. N., Dittmar, T., and Tranvik, L. J.: Persistence of dissolved organic matter in lakes related to its molecular characteristics, Nat. Geosci., 8, 454–457, 2015.

Kleeberg, A.: Impact of aquatic macrophyte decomposition on sedimentary nutrient and metal mobilization in the initial stages of ecosystem development, Aquat. Bot., 105, 41–49, 2013.

Koinig, K. A., Shotyk, W., Lotter, A. F., Ohlendorf, C., and Sturm, M.: 9000 years of geochemical evolution of lithogenic major and trace elements in the sediment of an alpine lake – the role of climate, vegetation, and land-use history, J. Paleolimnol., 30, 307–320, 2003.

Korsman, T., Nilsson, M. B., Landgren, K., and Renberg, I.: Spatial variability in surface sediment composition characterised by near-infrared (NIR) reflectance spectroscopy, J. Paleolimnol., 21, 61–71, 1999.

Kumke, T., Schoonderwaldt, A., and Kienel, U.: Spatial variability of sedimentological properties in a large Siberian lake, Aquat. Sci., 67, 86–96, 2005.

Lehtonen, T., Peuravuori, J., and Pihlaja, K.: Degradation of TMAH treated aquatic humic matter at different temperatures, J. Anal. Appl. Pyrol., 55, 151–160, 2000.

Leri, A. C. and Myneni, S. C. B.: Natural organobromine in terrestrial ecosystems, Geochim. Cosmochim. Ac., 77, 1–10, 2012.

Lidman, F., Kohler, S. J., Morth, C. M., and Laudon, H.: Metal Transport in the Boreal Landscape-The Role of Wetlands and the Affinity for Organic Matter, Environ. Sci. Technol., 48, 3783–3790, 2014.

Marbot, R.: The selection of pyrolysis temperatures for the analysis of humic substances and related materials .1. Cellulose and chitin, J. Anal. Appl. Pyrol., 39, 97–104, 1997.

McClymont, E. L., Bingham, E. M., Nott, C. J., Chambers, F. M., Pancost, R. D., and Evershed, R. P.: Pyrolysis GC-MS as a rapid screening tool for determination of peat-forming plant composition in cores from ombrotrophic peat, Org. Geochem., 42, 1420–1435, 2011.

Meredith, W., Snape, C. E., Carr, A. D., Nytoft, H. P., and Love, G. D.: The occurrence of unusual hopenes in hydropyrolysates generated from severely biodegraded oil seep asphaltenes, Org. Geochem., 39, 1243–1248, 2008.

Meyer-Jacob, C., Vogel, H., Boxberg, F., Rosen, P., Weber, M. E., and Bindler, R.: Independent measurement of biogenic silica in sediments by FTIR spectroscopy and PLS regression, J. Paleolimnol., 52, 245–255, 2014.

Meyers, P. A. and Ishiwatari, R.: Lacustrine organic geochemistry-an overview of indicators of organic matter sources and diagenesis in lake sediments, Org. Geochem., 20, 867–900, 1993.

Micić, V., Kruge, M., Körner, P., Bujalski, N., and Hofmann, T.: Organic geochemistry of Danube River sediments from Pančevo (Serbia) to the Iron Gate dam (Serbia-Romania), Org. Geochem., 41, 971–974, 2010.

Micić, V., Kruge, M. A., Köster, J., and Hofmann, T.: Natural, anthropogenic and fossil organic matter in river sediments and suspended particulate matter: A multi-molecular marker approach, Sci. Total Environ., 409, 905–919, 2011.

Mucci, A., Richard, L. F., Lucotte, M., and Guignard, C.: The differential geochemical behavior of arsenic and phosphorus in the water column and sediments of the Saguenay Fjord estuary, Canada, Aquat. Geochem., 6, 293–324, 2000.

Naeher, S., Gilli, A., North, R. P., Hamann, Y., and Schubert, C. J.: Tracing bottom water oxygenation with sedimentary Mn/Fe ratios in Lake Zurich, Switzerland, Chem. Geol., 352, 125–133, 2013.

Nguyen, R. T., Harvey, H. R., Zang, X., Van Heemst, J. D. H., Hetényi, M., and Hatcher, P. G.: Preservation of algaenan and proteinaceous material during the oxic decay of Botryococcus braunii as revealed by pyrolysis-gas chromatography/mass spectrometry and 13C NMR spectroscopy, Org. Geochem., 34, 483–497, 2003.

Nichols, J. E. and Huang, Y.: C23-C31 n-alkan-2-ones are biomarkers for the genus Sphagnum in freshwater peatlands, Org. Geochem., 38, 1972–1976, 2007.

Nierop, K. G. J. and Buurman, P.: Composition of soil organic matter and its water-soluble fraction under young vegetation on drift sand, central Netherlands, Eur. J. Soil Sci., 49, 605–615, 1998.

Ostrovsky, I. and Yacobi, Y. Z.: Organic matter and pigments in surface sediments: possible mechanisms of their horizontal distributions in a stratified lake, Can. J. Fish. Aquat. Sci., 56, 1001–1010, 1999.

Page, D. W.: Characterisation of organic matter in sediment from Corin Reservoir, Australia, J. Anal. Appl. Pyrol., 70, 169–183, 2003.

Peulvé, S., Sicre, M. A., Saliot, A., De Leeuw, J. W., and Baas, M.: Molecular characterization of suspended and sedimentary organic matter in an Arctic delta, Limnol. Oceanogr., 41, 488–497, 1996.

Plant, J. A., Kinniburgh, D. G., Smedley, P. L., Fordyce, F. M., and Klinck, B. A.: Arsenic and selenium, in: Environmental geochemistry: treatise on geochemistry, edited by: Lollar, B. S., Elsevier, Amsterdam, the Netherlands, 9, 17–66, 2005.

Rydberg, J.: Wavelength dispersive X-ray fluorescence spectroscopy as a fast, non-destructive and cost-effective analytical method for determining the geochemical composition of small loose-powder sediment samples, J. Paleolimnol., 52, 265–276, 2014.

Rydberg, J., Gälman, V., Ingemar, R., Bindler, R., Lambertsson, L., and Martinez-Cortizas, A.: Assessing the Stability of Mercury and Methylmercury in a Varved Lake Sediment Deposit, Environ. Sci. Technol., 42, 4391–4396, 2008.

Rydberg, J., Rosen, P., Lambertsson, L., De Vleeschouwer, F., Tomasdotter, S., and Bindler, R.: Assessment of the spatial distributions of total- and methyl-mercury and their relationship to sediment geochemistry from a whole-lake perspective, J. Geophys. Res.-Biogeo., 117, G04005, doi:10.1029/2012JG001992, 2012.

Santisteban, J. I., Mediavilla, R., Lopez-Pamo, E., Dabrio, C. J., Zapata, M. B. R., Garcia, M. J. G., Castano, S., and Martinez-Alfaro, P. E.: Loss on ignition: a qualitative or quantitative method for organic matter and carbonate mineral content in sediments?, J. Paleolimnol., 32, 287–299, 2004.

Sarkar, S., Wilkes, H., Prasad, S., Brauer, A., Riedel, N., Stebich, M., Basavaiah, N., and Sachse, D.: Spatial heterogeneity in lipid biomarker distributions in the catchment and sediments of a crater lake in central India, Org. Geochem., 66, 125–136, 2014.

Schellekens, J., Buurman, P., and Pontevedra-Pombal, X.: Selecting parameters for the environmental interpretation of peat molecular chemistry - A pyrolysis-GC/MS study, Org. Geochem., 40, 678–691, 2009.

Schulten, H. R. and Gleixner, G.: Analytical pyrolysis of humic substances and dissolved organic matter in aquatic systems: Structure and origin, Water Res., 33, 2489–2498, 1999.

Sessions, A. L., Zhang, L., Welander, P. V., Doughty, D., Summons, R. E., and Newman, D. K.: Identification and quantification of polyfunctionalized hopanoids by high temperature gas chromatography-mass spectrometry, Org. Geochem., 56, 120–130, 2013.

Sinninghe Damsté, J. S., Eglinton, T. I., and De Leeuw, J. W.: Alkylpyrroles in a kerogen pyrolysate: Evidence for abundant tetrapyrrole pigments, Geochim. Cosmochim. Ac., 56, 1743–1751, 1992.

Sobek, S., Algesten, G., Bergstrom, A. K., Jansson, M., and Tranvik, L. J.: The catchment and climate regulation of pCO$_2$ in boreal lakes, Glob. Change Biol., 9, 630–641, 2003.

Sobek, S., Zurbrugg, R., and Ostrovsky, I.: The burial efficiency of organic carbon in the sediments of Lake Kinneret, Aquat. Sci., 73, 355–364, 2011.

Ståhlberg, C., Bastviken, D., Svensson, B. H., and Rahm, L.: Mineralisation of organic matter in coastal sediments at different frequency and duration of resuspension, Estuar. Coast. Shelf S., 70, 317–325, 2006.

Stewart, C. E.: Evaluation of angiosperm and fern contributions to soil organic matter using two methods of pyrolysis-gas chromatography-mass spectrometry, Plant Soil, 351, 31–46, 2012.

Stubbins, A. and Dittmar, T.: Illuminating the deep: Molecular signatures of photochemical alteration of dissolved organic matter from North Atlantic Deep Water, Mar. Chem., 177, 318–324, 2015.

Taboada, T., Cortizas, A. M., Garcia, C., and Garcia-Rodeja, E.: Particle-size fractionation of titanium and zirconium during weathering and pedogenesis of granitic rocks in NW Spain, Geoderma, 131, 218–236, 2006.

Tesi, T., Langone, L., Goñi, M. A., Wheatcroft, R. A., Miserocchi, S., and Bertotti, L.: Early diagenesis of recently deposited organic matter: A 9-yr time-series study of a flood deposit, Geochim. Cosmochim. Ac., 83, 19–36, 2012.

Tjerngren, I., Meili, M., Bjorn, E., and Skyllberg, U.: Eight Boreal Wetlands as Sources and Sinks for Methyl Mercury in Relation to Soil Acidity, C / N Ratio, and Small-Scale Flooding, Environ. Sci. Technol., 46, 8052–8060, 2012.

Tranvik, L. J., Downing, J. A., Cotner, J. B., Loiselle, S. A., Striegl, R. G., Ballatore, T. J., Dillon, P., Finlay, K., Fortino, K., Knoll, L. B., Kortelainen, P. L., Kutser, T., Larsen, S., Laurion, I., Leech, D. M., Leigh McCallister, S., McKnight, D. M., Melack, J. M., Overholt, E., Porter, J. A., Prairie, Y., Renwick, W. H., Roland, F., Sherman, B. S., Schindler, D. W., Sobek, S., Tremblay, A., Vanni, M. J., Verschoor, A. M., Von Wachenfeldt, E., and Weyhenmeyer, G. A.: Lakes and reservoirs as regulators of carbon cycling and climate, Limnol. Oceanogr., 54, 2298–2314, 2009.

Trolle, D., Zhu, G. W., Hamilton, D., Luo, L. C., McBride, C., and Zhang, L.: The influence of water quality and sediment geochemistry on the horizontal and vertical distribution of phosphorus and nitrogen in sediments of a large, shallow lake, Hydrobiologia, 627, 31–44, 2009.

Tolu, J., Gerber, L., Boily, J. F., and Bindler, R.: High-throughput characterization of sediment organic matter by pyrolysis-gas chromatography/mass spectrometry and multivariate curve resolution: A promising analytical tool in (paleo) limnology, Anal. Chim. Acta, 880, 93–102, 2015.

Valdes, F., Catala, L., Hernandez, M. R., Garcia-Quesada, J. C., and Marcilla, A.: Thermogravimetry and Py-GC/MS techniques as fast qualitative methods for comparing the biochemical composition of Nannochloropsis oculata samples obtained under different culture conditions, Bioresource Technol., 131, 86–93, 2013.

Vancampenhout, K., Wouters, K., Caus, A., Buurman, P., Swennen, R., and Deckers, J.: Fingerprinting of soil organic matter as a proxy for assessing climate and vegetation changes in last interglacial palaeosols (Veldwezelt, Belgium), Quaternary Res., 69, 145–162, 2008.

Vogel, H., Wessels, M., Albrecht, C., Stich, H.-B., and Wagner, B.: Spatial variability of recent sedimentation in Lake Ohrid (Albania/Macedonia), Biogeosciences, 7, 3333–3342, doi:10.5194/bg-7-3333-2010, 2010.

Wagner, S., Jaffé, R., Cawley, K., Dittmar, T., and Stubbins, A.: Associations between the molecular and optical properties of dissolved organic matter in the Florida Everglades, a model coastal wetland system, Front. Chem., 3, 66, doi:10.3389/fchem.2015.00066, 2015.

Wakeham, S. G., Lee, C., Hedges, J. I., Hernes, P. J., and Peterson, M. L.: Molecular indicators of diagenetic status in marine organic matter, Geochim. Cosmochim. Ac., 61, 5363–5369, 1997.

Yin, H., Feng, X. H., Qiu, G. H., Tan, W. F., and Liu, F.: Characterization of Co-doped birnessites and application for removal of lead and arsenite, J. Hazard. Mater., 188, 341–349, 2011.

Zheng, Y. H., Zhou, W. J., and Meyers, P. A.: Proxy value of n-alkan-2-ones in the Hongyuan peat sequence to reconstruct Holocene climate changes on the eastern margin of the Tibetan Plateau, Chem. Geol., 288, 97–104, 2011.

Zhu, M. Y., Zhu, G. W., Li, W., Zhang, Y. L., Zhao, L. L., and Gu, Z.: Estimation of the algal-available phosphorus pool in sediments of a large, shallow eutrophic lake (Taihu, China) using profiled SMT fractional analysis, Environ. Pollut., 173, 216–223, 2013.